Graduate program

mbhd

University of Crete Medical School

FORTH

Institute of Molecular Biology and Biotechnology

University of Crete

Faculty of Medicine

Master Thesis:

"Functional analysis of Met18/MMS19 protein in transcription and DNA repair"

"Λειτουργική ανάλυση της πρωτεΐνης Met18/MMS19 στην μεταγραφή και την επιδιόρθωση του DNA".

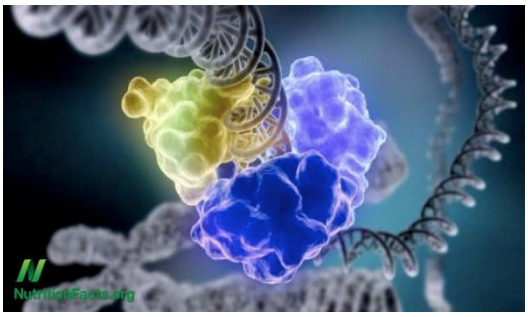

Masters Student: **Maria Stratigopoulou**

Τριμελής επιτροπή:

Γ. Γαρίνης

Χ.Σπηλιανάκης

Ι. Παπαματθαιάκης

Abstract

The somatic genome integrity is one of the most important functions of an organism and it must be preserved during its entire lifetime. For this reasons nature has invested heavily in genome maintenance by creating special apparatus, consisting of several sophisticated DNA damage repair systems that are all parts of the same puzzle, the DNA damage response (DDR), known as the cellular response to DNA damage. The importance of the study of the DDR can be understood by the relationship between genome stability and human health affected by many genome instability syndromes. Nucleotide excision repair (NER) is one of the DNA repair pathways that repairs cyclobutanepyrmidine dimers (CPDs and pyrmidine 6-4(6-4 PPs) that interfere with transcription and replication resulting from Ultraviolet irradiation (UV). The function of many proteins depends on various cofactors, including metal ions, including Fe–S clusters (Iron sulfur clusters).The mechanism, via which the transfer of Fe-S clusters to target Fe-S proteins, was unknown. According to recent studies, MMS19 has been found to interact physically with the Cytoplasmic Fe-S assembly (CIA) proteins, a multiprotein complex that mediates the incorporation of iron-sulfur cluster into apoproteins and is involved in the maturation of a subset of Fe/S proteins including those with functions in DNA repair, and telomere stability.

At present, any mechanistic understanding of how MMS19 functions in transcription and DNA repair remains elusive. Here, we develop a comprehensive and multidisciplinary approach to dissect the functional contribution of MMS19 in genome maintenance and gene expression regulation. Professor Garinis lab has recently generated Mmms19-/- mice; that were lethal at an early embryonic stage. For this purpose we aim to generate tissue specific knock out animals for MMS19, via the cre/flox system. Furthermore, in collaboration with Professor Alexandraki's lab we have used the *S. cerevisiae* to dissect the functional contribution of Met18 (MMS19) in DNA repair and transcription.

For the tissue specific knock out animals we generated ES cells transfected with a specific expression vector containing the MMS19 genomic region (1st exon) flanked by two LoxP sites. In yeasts, we constructed appropriately tagged and gene deleted strains of Met18 protein (*met18*Δ) and examined the effects of exposure to genotoxic stress. We also explored the role of Met18 in transcription indirectly, via studying the effect of its deletion, on Rad3 recruitment to its known targets and the recruitment of Met18 protein on the same gene targets. We also examined the effect of Met18 depletion on the expression of Rad3 target genes as well as its effect on Rad3 protein levels. It seems that Met18 depletion alone decreases the recruitment of the Rad3 to the promoters of the examined gene targets. Also the DNA damaging conditions lead to impaired recruitment of Rad3. Under both conditions the effect seems to be more severe (synergistic). Examination of Rad3 protein levels showed that UV irradiation does not affect the stability of the protein as its protein levels are not affected following UV exposure, but the depletion of Met18 decreases significantly the protein levels of Rad3. Finally, since we have found that the binding of Rad3 is affected in the *met18*Δ strain we also examined whether the expression of these gene targets was also decreased in the mutant strain in native conditions and following UV irradiation. Examination of the specific gene RNA accumulation showed

decreased expression levels of both *PYK1* and *ADH1* genes under both conditions (*met18*Δ,UV) emphasizing the role of Met18 in the transcription of these genes. From all the previous results we can conclude that Met18 depletion affects both the quantity (stability) of Rad3 protein and its functionality in transcription, not only its recruitment to its known targets, but also accumulation of their RNA. In order to reveal the general effect of Met18 depletion on the genome-wide Rad3 recruitment and transcriptional role we could do ChIP sequencing experiments and RNA-seq from the WT and *met18*Δ strains under both conditions (genotoxic stress, native).

Περίληψη

Η διατήρηση της ακεραιότητας του σωματικού γονιδιώματος σε όλη τη διάρκεια της ζωής ενός οργανισμού είναι μια από τις πιο σημαντικότερες λειτουργίες του. Για αυτό το σκοπό η φύση έχει επενδύσει σε μεγάλο βαθμό στην διατήρηση του γονιδιώματος αναπτύσσοντας ειδικές πρωτεϊνικές μηχανές, αποτελούμενες από εξειδικευμένα συστήματα επιδιόρθωσης του DNA και αυτοί οι μηχανισμοί αποτελούν τμήματα του ίδιου παζλ, γνωστό ως η απόκριση στις βλάβες του DNA (DDR). Η σημαντικότητα της μελέτης του DDR γίνεται αντιληπτή από την σχέση της γονιδιακής σταθερότητας και της ανθρώπινης υγείας, η οποία προσβάλλεται από σύνδρομα αστάθειας του γονιδιώματος. Το μονοπάτι επιδιόρθωσης μέσω εκτομής βάσης (NER) είναι ένα από τα μονοπάτια επιδιόρθωσης και εξειδικεύεται στην επιδιόρθωση διμερών πυριμιδίνης κυκλοβουτανίου (CPDs) τα οποία προέρχονται από την υπεριώδη ακτινοβολία (UV) και παρεμβαίνει στην αντιγραφή και την μεταγραφή του γονιδιώματος. Η λειτουργία πολλών πρωτεϊνών εξαρτάται από συμπαράγοντες, όπως τα μεταλλικά ιόντα, συμπεριλαμβανομένων και των ιόντων σιδήρου-θείου (Fe–S clusters). Ο μηχανισμός μεταφοράς των ιόντων αυτών στις πρωτεΐνες στόχους τους δεν ήταν γνωστός, αλλά σύμφωνα με πρόσφατες μελέτες η πρωτεΐνη MMS19 έχει βρεθεί να αλληλεπιδρά με το κυτταροπλασματικό σύμπλοκο συγκέντρωσης των ιόντων σιδήρου-θείου (CIA complex).Το πολυπρωτεϊνικό αυτό σύμπλοκο μεταφέρει τα Fe–S ιόντα στις από-πρωτεΐνες (πχ επιδιόρθωσης και σταθερότητας των χρωμοσωμάτων) και συμμετέχει στην ωρίμανση τους.

Μέχρι σήμερα ο μηχανισιμός της λειτουργίας της πρωτεΐνης MMS19 στην μεταγραφή και την επιοδιόρθωση του DNA παραμένει αναπάντητος. Για το σκοπό αυτό στοχεύουμε στην ανάπτυξη διεπιστιμονικής και αναλυτικής προσέγγισης για την μελέτη της λειτουργικής σημασίας της MMS19 στην διατήρηση του γονιδιώματος και στην ρύθμιση της γονιδιακής έκφρασης. Στο εργαστήριο του καθηγητή Γ.Γαρίνη έχουν αναπτυχθεί ποντίκια-μοντέλα με πλήρη έλλειψη του γονιδίου MMS19, των οποίων ο φαινότυπος είναι θανατηφόρος σε πρόωρο εμβρυονικό στάδιο. Για αυτόν τον λόγο, το εργαστήριο στοχεύει στην ανάπτυξη ζωικών μοντέλων με ιστοειδική έλλειψη αυτών των γονιδίων (Knock-out) μέσω του συστήματος cre/flox. Επίσης, σε συνεργασία με το εργαστήριο της καθηγήτριας Δ. Αλεξανδράκη έχουμε χρησιμοποιήσει τον σακχαρομύκητα ως μοντέλο-οργανισμό για την μελέτη της λειτουργίας της πρωτεΐνης Met18 (MMS19) στην μεταγραφή και την επιδιόρθωση του DNA.

Για την ανάπτυξη των ιστοειδικών ποντικών knock out έγινε διαμόλυνση εμβρυονικών βλαστοκυττάρων με φορείς έκφρασης του γονιδίου, το οποίο περιβάλλεται από τις

αλληλουχίες LoxP (στο πρώτο εξώνιο). Στον σακχαρομύκητα αναπτύξαμε στελέχη με επισήμανση (tag) ή γονιδιακή έλλειψη της Met18 (*met18*Δ) και εξετάσαμε την απόκριση τους σε γενοτοξικό στρες. Για την λειτουργική σημασία αυτής της πρωτεΐνης στην μεταγραφή μελετήσαμε την επίδραση της έλλειψης της στην στρατολόγηση της Rad3 στα γονίδια στόχους της και την πιθανή στρατολόγηση της Met18 στα ίδια γονίδια-στόχους. Επίσης, μελετήσαμε την επίδραση της στην έκφραση των γονιδίων-στόχων της Rad3 και στα πρωτεϊνικά επίπεδα της ίδιας πρωτεΐνης (Rad3). Σύμφωνα με τα αποτελέσματα μας, η έλλειψη της Met18 μειώνει την στρατολόγηση της Rad3 στα εξεταζόμενα γονίδια-στόχους της. Το ίδιο ισχύει και για τις γενοτοξικές συνθήκες. 'Ομως η δράση τους μοιάζει να είναι συνεργατική και να παρατηρείται μεγαλύτερη επίδραση στην στρατολόγηση της Rad3 κατά τον συνδυασμό των δύο συνθηκών (UV και *met18*Δ). Η UV ακτινοβολία δεν επιδρά στην πρωτεϊνική σταθερότητα της Rad3, καθώς τα επίπεδα της παραμένουν σταθερά μετά την έκθεση σε UV ακτινοβολία, ενώ η έλλειψη της Met18 οδηγεί στην μείωση τους. Τέλος, αφού ήδη είχαμε βρει, ότι η στρατολόγηση της Rad3 στα γονίδια στόχους της μειώνεται κατά την έλλειψη της Met18 (*met18*Δ) και σε συνθήκες UV, εξετάσαμε εάν μειώνεται και η έκφραση αυτών των γονιδίων-στόχων. Το αποτέλεσμα ήταν μειωμένη έκφραση των γονιδίων στόχων (*PYK1* και *ADH1)* και στις δύο συνθήκες, τονίζοντας τον ρόλο της Met18 στην μεταγραφή αυτών των γονιδίων. Από όλα τα παραπάνω αποτελέσματα μπορούμε να συμπεράνουμε ότι η έλλειψη της πρωτεΐνης Met18 επιδρά όχι μόνο στην σταθερότητα της πρωτεΐνης Rad3 αλλά και στην λειτουργικότητα της κατά την μεταγραφή, τόσο στην στρατολόγηση της στα γονίδια στόχους της όσο και στην έκφραση τους. Για να ανακαλύψουμε την γενική επίδραση της έλλειψης της Met18 στην στρατολόγηση της Rad3 σε ολόκληρο το γονιδίωμα και τον μεταγραφικό της ρόλο, χρειάζονται πειράματα ανοσοκατακρήμνισης χρωματίνης και αλληλούχισης (ChIP sequencing) και αλληλούχισης του RNA (RNA-seq) από φυσιολογικά στελέχη και από *met18*Δ στελέχη σε φυσιολογικές συνθήκες και σε συνθήκες γενοτοξικού στρες.

Introduction

DNA Damage and DNA damage response

Cells are composed of complex chemical machineries that include all the biomolecules (proteins, lipids and nucleic acids).All the parts of these machineries are subject to indiscriminate damage caused by spontaneous reactions (mostly hydrolysis) and by numerous endogenous and exogenous reactive agents. DNA is the most important macromolecule since all other macromolecules are renewable, while DNA is irreplaceable; the errors acquired in DNA are permanent and may have irreversible consequences. Cellular function depends on the integrity of the somatic genome. Since the somatic genome integrity must be preserved during the entire lifetime of an organism nature has invested heavily in genome maintenance by creating special apparatus, consisting of several sophisticated DNA damage repair, tolerance and checkpoint systems, as well as effector machinery that enables cell survival or triggers senescence or cell death when DNA is damaged. The faithful transmission of the genetic information for extended time periods is ensured by the aforementioned mechanisms. All the aforementioned mechanisms and signaling pathways are parts of the same puzzle, the DNA damage response (DDR) known as the cellular response to DNA damage.

The sources of DNA damage can be separated in endogenous and exogenous. The basic endogenous enemy of genome integrity is organism's metabolism that is responsible for the production of reactive oxygen species (ROS) and their subsequent products. Basic exogenous sources of DNA damage are UV and ionizing radiation, and numerous chemicals. Different sources of damage can induce different kind of DNA damage and different DNA repair mechanisms (Figure 1). Double strand breaks (DSBs) can result from ionizing radiation, radiomimetic drugs or ROS. The DNA repair mechanisms that are responsible for the repair of this type of damage are Non-homologous end joining (NHEJ) and Homologous end joining (HE). Ionizing irradiation can also lead to single strand breaks (SSBs) which are repaired by different repair systems the single strand breaks repair (SSBRs).It is estimated that thousands of single-stand breaks and spontaneous base losses occur daily in the nuclear genome of every cell[1][2]. Together with other types of spontaneous damage, the total may amount to about 100,000 lesions per cell per day[2].It is likely that this number increases considerably under certain conditions; for example, a single day in the sun may induce up to 100,000 UV photoproducts in each keratinocyte [3].

UV radiation can induce cyclobutanepyrmidine dimers (CPDs and pyrmidine 6-4(6-4 PPs) that interfere with transcription and replication. One of the main mechanisms that cells have evolved in order to maintain the genome integrity is the evolutionary conserved repair mechanism known as NER (nucleotide excision repair). This

pathway is the principal repair mechanism that is responsible for the repair of bulky helix-distorting damage, such as lesions induced by UV light.

The importance of the study of the DDR can be understood by the relationship between genome stability and human health. There are many genome instability syndromes, typically characterized by progressive degeneration of specific tissues; cancer predisposition, chromosomal instability, and hypersensitivity to DNA damaging agents [2] and [3] (figure 1 DNA damage response syndrome).

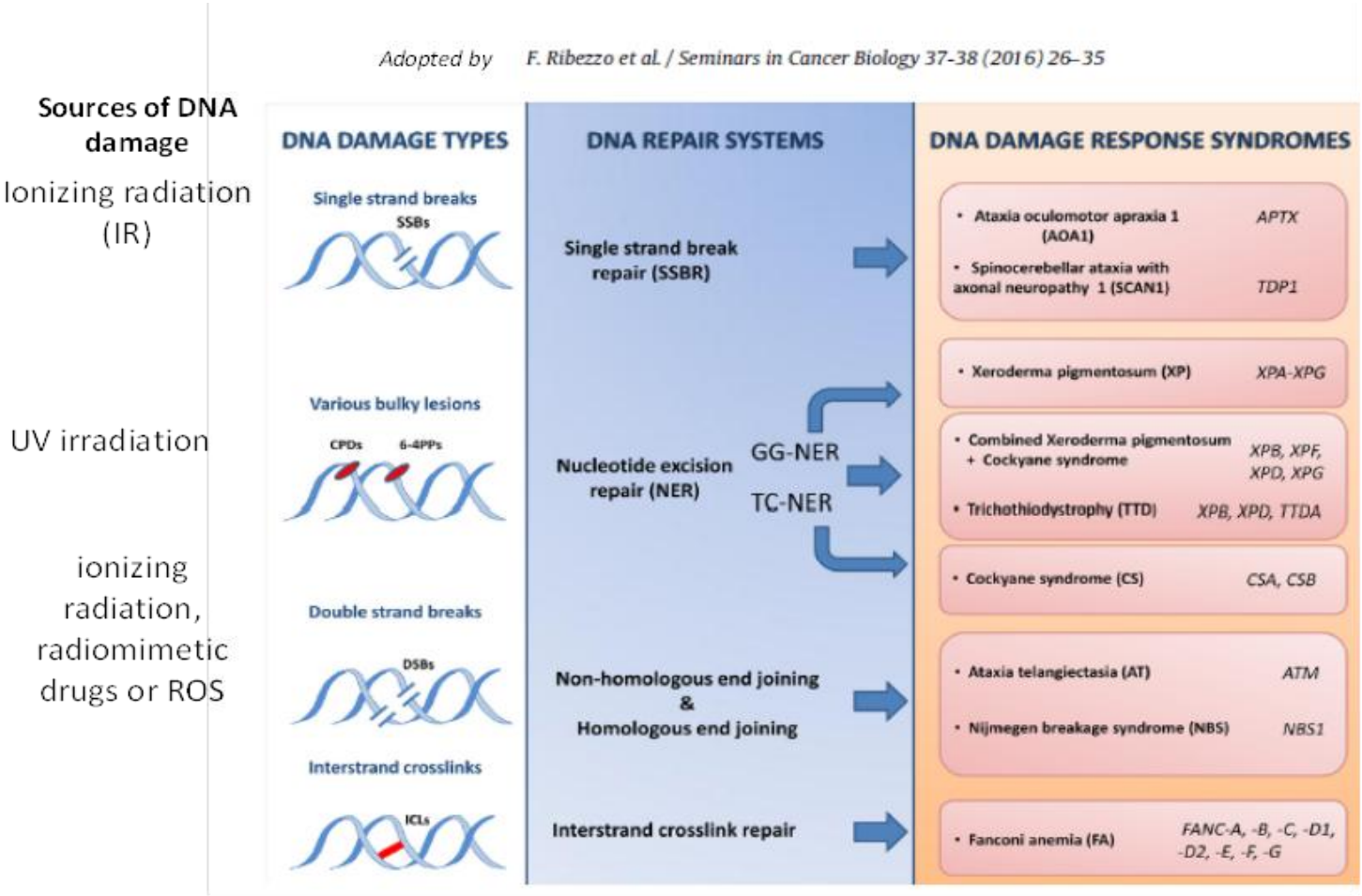

Figure 1: Endogenous and exogenous sources of DNA damage induce different types of DNA damage and for their repair different repair systems are presented. The human disorders coming from DNA damage response defects are illustrated. Double strand breaks (DSBs) can result from ionizing radiation, radiomimetic drugs or ROS. The DNA repair mechanisms that are responsible for the repair of this type of damage are Non-homologous end joining and Homologous end joining. Ionizing irradiation can also lead to single strand breaks (SSBs) which are repaired by different repair systems the single strand breaks repair (SSBRs).

UV radiation can induce cyclobutanepyrmidine dimers (CPDs and pyrmidine 6-4(6-4 PPs) that interfere with transcription and replication repaired by NER.

Nucleotide Excision Repair (NER)

NER can be distinguished into different subpathways according to the distortions that recognizes and removes: the subpathway that is active throughout the genome (i.e., global genome repair, GGR), and the subpathway that acts selectively at the transcribed strand of active genes (i.e., transcription coupled repair, TCR)[4].
As far as the first subpathway is concerned the survey of the DNA is accomplished by the xeroderma pigmentosum, complementation group C (XPC)-RAD23-centrin, EF hand protein, 2 (CETN2) complex [5], and the UV damaged DNA-binding protein (UV-DDB) complex(DDB1-DDB2-containing E3-ubiquitin ligase complex). After the binding of the damaged DNA by the complex, RAD23 dissociates from XPC and does not participate in the remaining NER process[6]. Transcriptional factor II H (TFIIH) is a 10/11-subunit complex which, participates together with XPD in addition to the Cdk-activating kinase (CAK) complex and XPG in the process of unwinding the DNA around a lesion and stabilizing the single-stranded DNA [7].CAK is released from the core during the NER reaction. XPB has an ATPase activity that is responsible for the unwinding of the DNA and for the formation of a 27-nucleotide bubble asymmetrically flanking the damage [8]. The stabilization of the damaged DNA takes place by the proteins XPA and replication protein A (RPA), XPB and XPD [10]. The following step for the repair is the cleavage of the damaged DNA by specific endonucleases that are activated by RPA. These structure-specific endonucleases are XPG and excision repair cross-complementing rodent repair deficiency, complementation group 1 (ERCC1)-XPF, endonucleases that cleave the 30 and 50 side of the 24–32-nucleotide fragment containing the damaged DNA. RPA is then released from DNA to initiate new incision events. The filling of the single-strand gap is then filled by the replicative DNA polymerases d and e or the translesion DNA polymerase k. proliferating cell nuclear antigen (PCNA) loaded onto the DNA by replication factors C (RFC) and A stimulates the polymerase activity of the DNA polymerases d and e or the translesion DNA polymerase k [2].The nascent DNA fragment is finally sealed by DNA ligase IIIXRCC1 and DNA ligase I [4].
The way that damage recognition takes place in the other side of the NER pathway of NER, TCR, damage recognition requires RNA polymerase II (RNAPII). At the damaged DNA template RNAPII is stalled and bound to the damaged template during assembly of the TCR complex. Except from stalled RNAPII the TCR complex contains Cockayne syndrome B (CSB), a DNA dependent ATPase and CSA, a protein that is part of an E3-ubiquitin ligase complex [containing DDB1, Cullin 4A, and ring-box 1 (ROC1/Rbx1)]. The assembly of the other NER factors is initiated by the binding of CSB to stalled RNAPII. After the assembly of CSA and CSB it's the turn of the recruitment of CSA recruits(together with CSB) the nucleosomal binding protein high mobility group nucleosome binding domain 1 (HMGN1), XPA binding protein 2

(XAB2) and TFIIS. Once chromatin is accessible for TCR, the lesion is removed by the core NER reaction [4]**(Figure 2**).

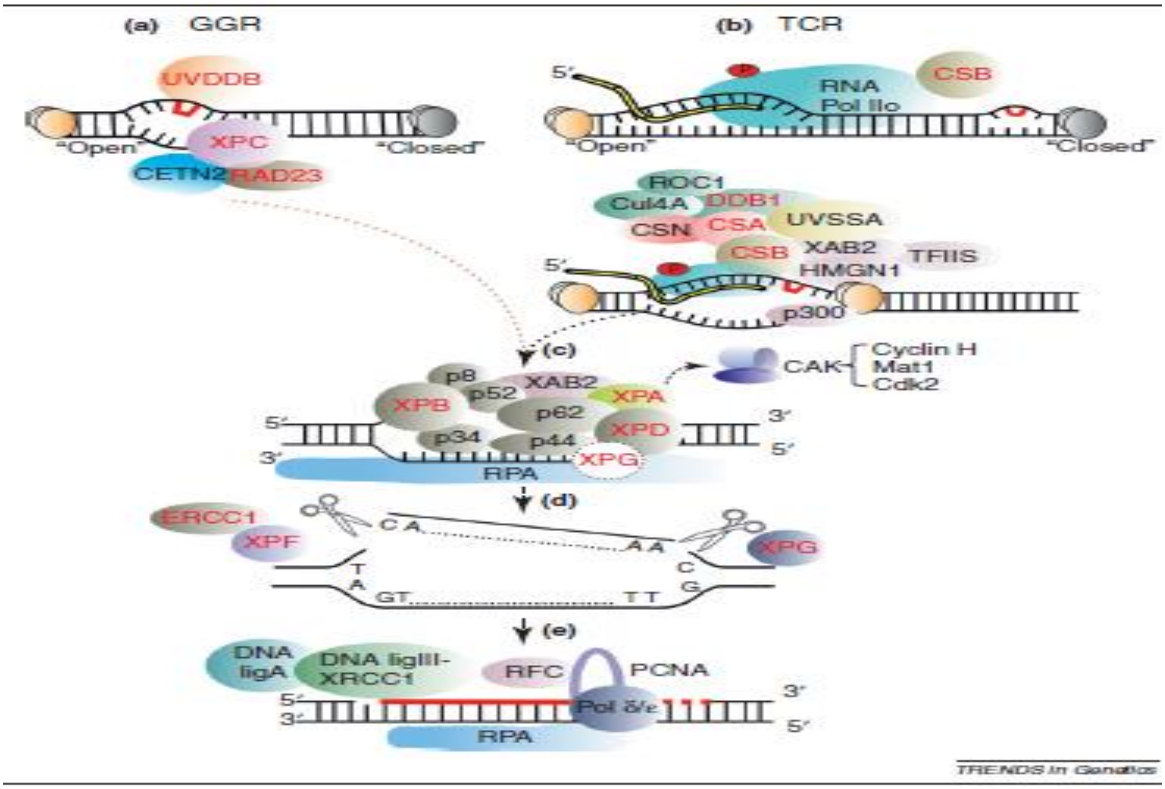

Figure2: The nucleotide excision repair (NER) mechanism in mammals. (a)During Global genome NER (GGR) helical distortions throughout the entire genome are recognized and removed. The helical distortions that occur specifically at the transcribed strand of active genes are selectively recognized and removed by the Transcription-coupled repair (TCR). The difference between the two sub pathways of NER, GGR and TCR lies only in how helix-distorting DNA lesions are recognized. After the step of recognition of damage, the two sub-pathways merge into common mechanisms that include the unwinding of DNA around the lesion (c), the stabilization and excision of the damaged DNA fragments (d), and finally the filling in and ligation of the single strand gap (e).

NER in *S. cerevisiae*

The contribution of studies in the budding yeast *Saccharomyces cerevisiae* as a model organism is important in elucidating the core NER mechanism in eukaryotes and has shed light into the functions of a multitude of NER proteins[9]. Many cellular processes and NER factors exhibit high conservation from yeast to humans. Most of the NER proteins have orthologs in humans, yeast, and other eukaryotes **(Table 1)**.

Table 1

S. cerevisiae	Human homolog or counterpart	Function(s)	Reference
Rad4	XPC	DNA damage recognition and binding	(Guzder et al. 1998)
Rad23	hRAD23B	Interacts with and stimulates Rad4	(Guzder et al. 1998)
TFIIH	TFIIH	DNA helicase activity mediates helix opening	(Egly and Coin 2011)
Mms19	MMS19L	Stabilizes XPD subunit of TFIIH	(Kou et al. 2008)
Rad14	XPA	Stabilizes preincision complex; lesion recognition	(Guzder et al. 2006)
Rpa	RPA	Stabilizes open single stranded DNA; damage recognition	(Guzder et al. 1995)
Rad2	XPG	Catalyzes 3′ incision; stabilizes open complex	(Habraken et al. 1993)
Rad10	ERCC1	Catalyzes 5′ incision; forms complex with Rad1	(Sung et al. 1993; Tomkinson et al. 1994)
Rad1	XPF	Catalyzes 5′ incision	(Sung et al. 1993; Tomkinson et al. 1994)
Rad26	CSB	TCR-specific factor; DNA-dependent ATPase	(van Gool et al. 1994)
Rpb9	Rpb9	TCR-specific factor; subunit of RNA polymerase II	(Li and Smerdon 2002)
Rad7-Rad16	DDB1-DDB2	GGR-specific factor; damage recognition; ubiquitinates Rad4	(Gillette et al. 2006; Ramsey et al. 2004; Reed 2005; Verhage et al. 1994)
Elc1	Elongin C	GGR-specific factor; forms complex with Rad7-Rad16	(Lejeune et al. 2009; Ramsey et al. 2004)
DNA polymerase δ	DNA polymerase δ	Gap-filling repair synthesis	(Wu et al. 2001)
DNA polymerase ε	DNA polymerase ε	Gap-filling repair synthesis	(Wu et al. 2001)
PCNA	PCNA	Sliding clamp for DNA polymerase δ	(Huang et al. 1998)
Cdc9	DNA ligase I	Ligation	(Wu, Braithwaite, and Wang 1999)

GGR in *S. cerevisiae*

The yeast homolog of human XPC is Rad4 and it is essential for both subpathways of NER in yeast, whereas in humans it is indispensable only for GGR[10]. In *S. cerevisiae*, the proteins specifically required for GGR are Rad7, Rad16, and Elc1[11]. More specifically, two of them are in complex, the Rad7-Rad16 complex, which binds specifically to UV-damaged DNA in an ATP-dependent manner [12]. This complex seems to have functional similarities with the DDB1-DDB2 (XPE) complexes [for a review see, (Reed 2005)]. It was also found that this complex exhibits a DNA dependent ATPase activity, which is inhibited when the complex comes across DNA damage [13]. A model for the activity of the Rad7-Rad16 complex was proposed, according to which the Rad7-Rad16 complex may act as an ATP dependent motor which translocates along, searching for damaged sites. When the complex finds

them it is stalled, and may remodel and open damaged chromatin, thereby facilitating recruitment of other NER factors [13]. The same model also proposes that the priority of this complex is to arrive first on the damaged sites in non-transcribed regions of the genome. These sites may serve as the nucleation sites for the recruitment of the other NER factors.

TFIIH and Rad3/XPD

As far as TFIIH, it is homolog with the human TFIIH complex and it is involved transactivation, the cell cycle, and nucleotide excision repair (NER) [14];[15]). Its structure has been studied with low resolution models for the yeast [16] and human complexes. TFIIH is composed of the core and the CDK-activating kinase module (CAK) [17].

Furthermore, TFIIH is composed of ten subunits highly conserved from yeast to mammals (**Figure 3a and 3b**)[18]. Ssl2/XPB and Rad3/XPD are helicases involved in NER and in transcription initiation. XPD exhibits an additional structural role, a bridge between the core and CAK modules of TFIIH [19]. Its activity in transcription initiation is mediating by anchoring the CAK module [20]. When these helicases are mutated can result in human autosomal recessive disorders such as xeroderma pigmentosum (XP), Cockayne syndrome (CS), and trichothiodystrophy (TTD). These syndromes are due to defects in TFIIH, which might affect not only NER, but also transcription [15].

a) 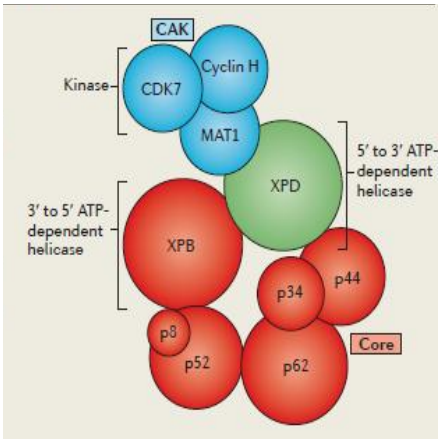

b) 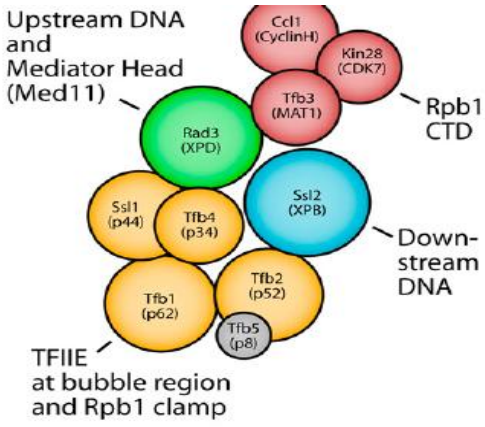

Figure 3: a) The mammalian TFIIH subunits are illustrated. They are separated in two main functional subcomplexes: the core complex and the CAK (cyclin-dependent kinase (CDK)-activating kinase) complex. In the first complexes six subunits (xeroderma pigmentosum group B complementing protein (XPB), p62, p52, p44, p34 and p8) are included. While in the second subcomplex there are the following proteins: CDK7, cyclin H and MAT1.XPD is the bridge between the core and CAK subcomplexes. There is also interaction between XPD and p44 (subunit of the core) and between XPD and MAT1 (subunit of the CAK. b) A model of the

yeast TFIIH complex. The human homologs of the TFIIH subunits are illustrated in brackets. The functional role of all the subunits of the TFIIH in both human and yeasts is transcribed in table 2.

Table 2 | Composition and function of the human and yeast TFIIH complex

TFIIH subcomplex	Human	Yeast	Function	Human genetic disorders
Core	XPB	Ssl2	3′ to 5′ ATP-dependent helicase	Trichothiodystrophy and combined xeroderma pigmentosum and Cockayne syndrome
	p62	Tfb1	Structural function and interacts with transcription factors and NER factors	
	p52	Tfb2	Regulates the XBP ATPase activity	
	p44	Ssl1	E3 ubiquitin ligase (in yeast)	
	p34	Tfb4	Structural function and strong interaction with p44	
	p8	Tfb5	Regulates the XBP ATPase activity	Trichothiodystrophy
XPD	XPD	Rad3	5′ to 3′ ATP-dependent helicase and forms a bridge between the CAK and the core	Trichothiodystrophy, xeroderma pigmentosum and combined xeroderma pigmentosum and Cockayne syndrome
CAK	CDK7	Kin28	Kinase	
	Cyclin H	Ccl1	Modulates the CDK7 kinase activity	
	MAT1	Tfb3	CAK stabilization and regulates cullin neddylation (in yeast)	

TFIIH functional role in transcription and DNA repair

TFIIIH is also involved in transcription and more specifically the transcription mediated by the RNA pol II. Its role in this process is to function as a basal factor working at the initiation, promoter escape and early elongation steps [21] but also in transcription re-initiation after RNA Pol II pausing [22].

Different subunits of TFIIH have different tasks during the process. One of their tasks is to open the DNA around the transcriptional start site (TSS).So the opening of DNA is mediated by the ATPase activity of XPB. The next of the process is the phosphorylation of the Rpb1 subunit of RNA Pol II by the cdk7 subunit of the CAK at the carboxyl-terminal domain (CTD) II[23][24]. The CTD can be phosphorylated in different amino acids of the repetitive amino acidic motif “YSPTSPS” according to different stages of transcription. For example cdk7 phosphorylates the CTD in Serine 5 during transcription initiation. This activation is eliminated by a phosphatase known as Rtr1 during elongation [25]. The fine tuning of transcription can be

regulated by the enzymatic activities of two subunits of the TFIIH which are XPB and Cdk7. The modulation of the enzymatic activity of XPB is mediated by TFIIE which is another basal transcription factor[26]. the transcription initiation is regulated by the cdk8 subunit of the Mediator by modulating the Cdk7 kinase activity by phosphorylating cyclin H, which impedes the activity of Cdk7 and inhibits transcription initiation [27].
TFIIH is not fully dedicated to the basal and activated RNA Pol II transcription but it is also implicated in the transcription of ribosomal DNA by RNA Pol I and it has been found to nucleoli at sites of active rDNA transcription [28],[29] and addition of TFIIH in a reconstituted RNA Pol I-dependent system stimulates transcription [28], although the role of TFIIH in this process still remains unclear.
TFIIH functions in DNA repair in a stepwise manner. Firstly, the binding of TFIIH to the damaged DNA takes place after the stimulation of the ATPase activity of XPB. This process is regulated by the interaction between TTDA, p52 and XPB[30]. Genotoxic agents lead to stronger interaction between TTDA, p52 and XPB and thus to increased ATPase activity of XPB [31].The second step after the binding of the TFIIH to the damaged DNA is the unwinding of DNA around the lesion by the helicase activity of XPD. The helicase activity of XPD is regulated by the interaction between p34, p44 and XPD[32].

The independent parts of TFIIH?

According to purification studies TFIIH can be sub divided in different subcomplexes
More specifically, TFIIH was resolved into four sub-complexes: the CAK, the core TFIIH and two other sub-complexes in which XPD was found associated with either the kinase complex or with the core TFIIH.
So XPD can be found in different subcomplexes and a possible explanation could be its implication in different processes except from transcription and repair. This hypothesis was proven by the purification of the CAK-XPD subcomplex that is involved in the coordination and progression of mitosis during the late nuclear division steps [33][34].
The regulative role of XPD in transcription is the embedded on regulating the CAK distribution within the cell after interacting with it. The relocalization of CAK explains how the complex can regulate its activity during cell cycle.

There is another complex of XPD independent of TFIIH and it is consists of XPD, MMS19, MIP18, Ciao1, and ANT2, MMXD. This has been found in the mitotic spindle and it participates in the correct chromosome segregation and nuclear shape formation. This complex is also discussed further in the part about the correlation of TFIIH and MMS19[35].

TCR in *S. cerevisiae*

The stalled Pol II due to lesions in the transcribed strand of a gene has been proposed to be the triggering step of TCR in eukaryotic cells[36][37].
Rad26, the yeast homolog of human CSB and a putative transcription repair coupling factor, is important for TCR but dispensable for GGR. However, TCR in yeast is not solely dependent on Rad26, as a significant amount of repair still occurs in cells lacking Rad26 [38]. Rpb9, a nonessential subunit of Pol II, has also been shown to play a role in mediating TCR [38].
Rad26- and Rpb9- mediated TCR subpathways have been shown to have different efficiencies in different regions of a gene [39]. Rpb9- mediated TCR operates more effectively in the coding region than in the region upstream of the transcription start site; whereas the Rad26-mediated subpathway operates equally well in both regions [38]. Additionally, in log phase wild type cells, the relative contributions of these two subpathways of TCR may be different from gene to gene. The different contributions of the two subpathways of TCR in different genes may be caused by different levels of transcription. Rad26- and Rpb9-mediated repair are also differently modulated by different promoter elements[39]. The coupling of Rad26-mediated repair with transcription depend on the levels of transcription, meaning that in case of substantial transcription the Rad26-mediated repair is transcription-coupled, whereas in case of low levels of transcription it is transcription-independent. There is evidence suggesting that Rbp9-mediated TCR is strictly coupled to transcription. It takes place only in the transcribed strand and is efficient only if the TATA and UAS sequences are present [39].

Iron sulfur clusters (Fe-S) biogenesis

The function of many proteins depends on various cofactors, including metal ions. The oldest and most versatile inorganic cofactors are probably Fe–S clusters. Fe–S clusters were discovered in the early 1960s by purifying enzymes with characteristic electron paramagnetic resonance signals. Plant and bacterial ferredoxins and respiratory complexes I–III of bacteria and mitochondria, were the first Fe-S proteins discovered. There are several functions of the Fe-S clusters. One of their functions is their role as electron donors or acceptors. They have also been implicated in the regulation of gene expression by sensing the environmental or intracellular condition. They also function in enzymatic catalysis or they can even have structural role.
In striking contrast to the chemical simplicity of Fe–S clusters, their biosynthesis *in vivo* appears to be a rather complex and coordinated reaction.

There is a conserved biosynthetic pathway for the synthesis of Fe/S clusters (iron sulfur) and their assembly into proteins as inorganic cofactors. The first step of iron sulfur biosynthesis takes place in the mitochondria. More specifically, mitochondrial Fe/S proteins are matured by the iron-sulfur cluster (ISC) assembly machinery. The next step of this process takes place in the cytoplasm, where ISC and iron-sulfur cluster assembly (CIA) machinery, transfer the Fe-S compound to the other proteins. The crucial role of the ISC and CIA systems and of proper Fe-S cluster assembly is pointed by their high conservation in eukaryotes, from yeast [40].The transport of the Fe-S clusters from the mitochondria to the cytoplasm depends on the ABC transporter Atm1 (ABCB7 in humans) and on the sulphydryl oxidase Erv1 (**Figure 4**).
In yeast the first step for the assembly of Fe-S clusters takes place on the scaffold proteins cytosolic Fe-S cluster assembly factors NBP35 (Nbp35) and CFD1 (Cfd1) of the CIA machinery. In this complex there is a transient bond [4Fe-4S]. This step also requires Fe-S cluster assembly protein DRE2 (Dre2) [41].Subsequently, the labile Fe-S cluster is transferred to a complex of two proteins: cytosolic Fe-S cluster assembly factor NAR1 (Nar1) and the WD40-repeat protein, cytosolic Fe-S assembly protein 1 (Cia1). The last step of this process is the transfer of Fe-S clusters and their incorporation in target proteins. The target proteins are then named as holoproteins. The homolog subunits of the CIA machinery in mammals have also been studied. The mammalian CIA system is composed of CIAO1 (homolog of Cia1), CIAPIN1 (Dre2 homolog), cytosolic Fe-S cluster assembly factor NARFL (Nar1 homolog), cytosolic Fe-S cluster assembly factor NUBP1 (Nbp35 homolog), and cytosolic Fe-S cluster assembly factor NUBP2 (Cfd1 homolog) have been identified as components of the CIA system in mammals [40].

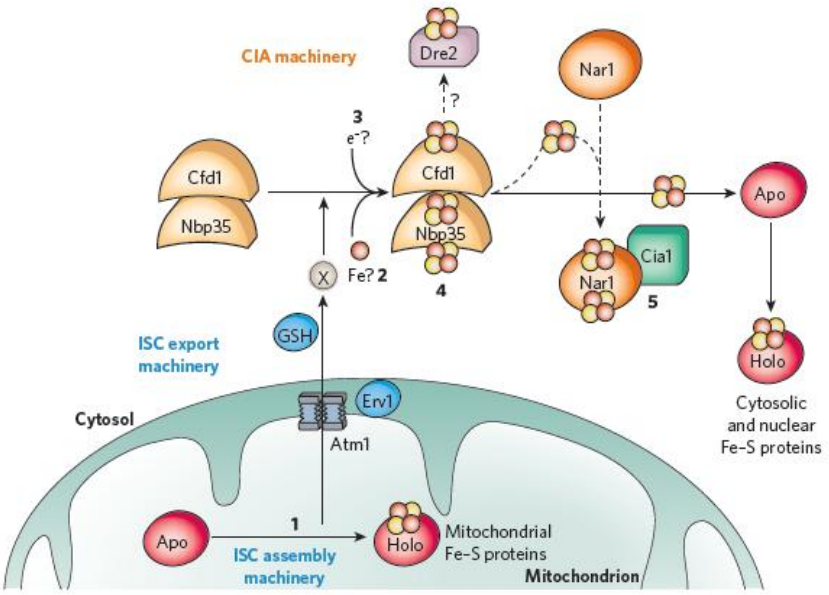

Figure 4: The roles of mitochondria and the CIA machinery in Fe–S-protein biogenesis in the cytosol and nucleus of eukaryotes.

Atm1, which is an ABC transporter of the mitochondrial inner membrane exports an unknown compound (X) to the cytosol for use in Fe–S-protein assembly, and is assisted by the tripeptide glutathione (GSH) and the intermembrane-space sulphydryl oxidase Erv1, which introduces disulphide bridges into substrates. In the cytosol, Fe–S-protein maturation takes place in to main steps and is mediated by the components of the CIA machinery catalyse First, Fe–S clusters are assembled on the P-loop NTPase complex Cfd1–Nbp35. During the next step of the process Fe–S clusters bound to Cfd1–Nbp35 are labile and can be transferred to cytosolic and nuclear apoproteins (Apo) helped by the iron-only hydrogenase-like protein Nar1 and the WD40-repeat proteinCia1.

Functional role of iron and iron sulphur compounds (Fe-S)

The physiology of many organisms is affected by the unbalanced levels of the iron levels. Increased levels of iron can be source of Reactive Oxygen Species (ROS) production. ROS can result in damaged lipids, DNA and proteins leading to genome instability and cell death. On the contrary, decreased levels of iron can result in anemia, which is one of the major public health problems. Iron is the cofactor of numerous of proteins involved in very important cell functions such as, DNA replication and repair. The regulatory role of iron in cell cycle is known by the cell cycle arrest during intracellular iron disruption. Most of the ISC and CIA components are essential for the viability of the yeast and human cells. The diseases caused by defects in Fe–S-protein biogenesis components or Fe–S proteins highlight the central importance of Fe–S-protein biogenesis in mammals. For example, mutations in the putative human Fe–S proteins XPD and FANCJ cause multiple disease phenotypes including xeroderma pigmentosum and Fanconi anaemia.

MMS19

MMS19 gene codes a protein (MMS19) which is highly conserved among the species from yeast to humans. More specifically, the homology of the yeast protein with the human MMS19 is 25%. Alignment of the translated sequences of MMS19 from multiple eukaryotes, including mouse and human, revealed the presence of several conserved regions. One of these regions, that the family of MMS19 proteins is characterized, is a conserved domain in the C terminus known as, the HEAT repeat, which usually contains 30-34 amino acids. The structure of this domain, according to data from crystallography experiments is characterized by two a-helices separated by a short loop. Many proteins are characterized by these HEAT motifs, some of them are implicated in the formation of multiprotein complexes, such as microtubules. These HEATS repeats have also been found in chromatin–associated proteins and in transcription regulating proteins.[42]

The role of MMS19 (also known as MET18 in yeast) in yeasts has been studied by the development of mutant strains. These strains have exhibited several defects in different cellular processes including methionine synthesis, sensitivity to genotoxic

stress, and the presence of extended telomeres [10][43][44]. However the mechanistic explanation of all these diverse cellular roles is still unknown. One more known phenotype of yeast met18Δ strains is that they exhibit defects in both subpathways of NER (TC-NER and GGNER) [45]. Also it has been found a thermoliabile defect in RNA Pol II transcription that in extracts from *met18*Δ strain.

The mechanism, via which the transfer of Fe-S clusters from the CIAO1-NARFL complex to target Fe-S proteins, was unknown. According to recent studies, in yeast cells it has been found to interact physically with the Cytoplasmic Fe-S assembly (CIA) proteins and is involved in the maturation of a subset of Fe/S proteins including those with functions in DNA replication, DNA repair, and telomere stability[46].More specifically, MMS19 has been found to interact with CIA1[46] and CIA2[46][47] protein subunits of the CIA machinery S.*cerevisiae* by both high throughput experiments and were also manually curated (Yeast two hybrid Affinity purification followed by mass spectrometry and Affinity Capture-Western blot respectively).Moreover, both the human and yeast MMS19 proteins interact with numerous Fe-S proteins, including Pol δ, DNA primase, Dna2, XPD, RTEL1 and FANCJ[48]. In S.*cerevisiae* Met18 protein has been found to interact physically with 24 proteins but only five of them have been found in more than one study. These are CIA1, CIA2 and RAD3, UB14 and SSB1. According to different studies, there are nuclear proteins that met18 has been found to interact with them. These proteins are SPC24, RPC40, MED11, BCY1, RAD3, NTG2, DNA2, but none of them has been found to interact with Met18 in more than one study.
Furthermore, in the absence of MMS19, the stability and incorporation of iron into Fe-S proteins is reduced, suggesting that MMS19 is an important factor in the assembly of cytosolic Fe-S cluster proteins [48]. This physical interaction between Fe/S proteins and MMS19 (and its putative functional partners CIAO1 and FAM96B) may link the function between Fe/S cluster synthesis and insertion into apoproteins. This conserved function of MMS19 can explain many, if not all, of the previously described phenotypes associated with MMS19 defects (**Figure 5**) [46].Moreover, both the human and yeast MMS19 proteins interact with numerous Fe-S proteins, including Pol δ, DNA primase, Dna2, XPD, RTEL1 and FANCJ. [48]
We can conclude that the pleiotropic phenotypes of the deletants of Met18 are explained by its role in Fe-S incorporation in a wide range of proteins with functions in different cellular processes.

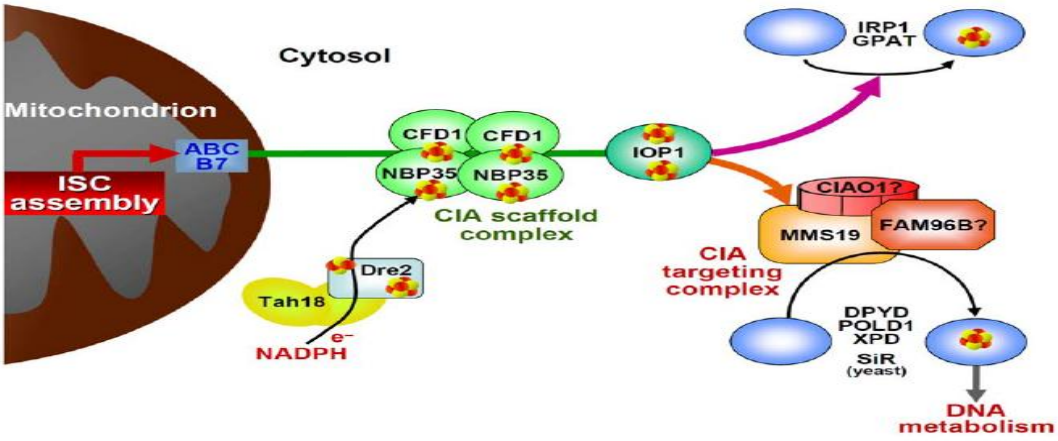

Figure5: Model for MMS19 function in maturation of Fe/S proteins involved in DNA metabolism. Fe/S protein biogenesis requires the mitochondrial ISC assembly machinery, the ABC transporter ABCB7 and the CIA machinery. The CIA component MMS19 is part of the 'CIA targeting complex' that transfers Fe/S clusters from the CIA scaffold complex CFD1-NBP35 to specific Fe/S apoproteins including members involved DNA metabolism. The putative roles of human CIAO1 and FAM96B in the assembly process remain to be elucidated.

In *S.pombe* it was found to interact with a silencing complex containing Dos1, Rik1, and cdc20 (polye subunit). This complex is involved in DNA replication and heterochromatin assembly. Its localization was predominantly nuclear. In the strain with disrupted the expression of met18/Mms19 the levels of siRNAs were decreased, meaning that it is involved in the regulation of centromeric transcription. They had also observed decreased accumulation of RNApolII in the same strain. They concluded that MMS19 is a transcriptional activator required for RNA polII mediated transcription of the heterochromatin.

During G1/S phase, while synthesizing the leading heterochromatin strands, Cdc20 regulates heterochromatin transcription by interacting with Mms19, and it also recruits Dos2 and Rik1. Another DNA polymerase subunit may be responsible for a similar process on the lagging strand. Heterochromatin transcripts are subsequently processed into siRNAs by the RNA-induced transcriptional silencing (RITS) complex. During late S phase, the complex containing Dos1, Dos2 and Rik1, together with the siRNAs, promotes H3K9 methylation by Clr4. During G2 phase, Swi6 binds to methylated H3K9 to reassemble chromatin into a repressed state and retain cohesion [49].

In mammalian cell lines it has been found that MMS19 is in protein complex with XPD but not with the other subunits of the TFIIH. According to the same study MMS19 was found in complex with the FAM96B/ (MIP18), Ciao1, and ANT2. It was also claimed that, siRNA-mediated knockdown of MMS19, MIP18, or XPD can lead to

improper chromosome segregation and accumulation of nuclei with abnormal shapes.[35].

Another more recent study revealed that XPD associates with the CIA targeting complex or TFIIH in two mutually exclusive protein complexes. Blocking Fe-S cluster assembly on XPD inhibits its incorporation into TFIIH. The conclusion of this study is that XPD maturation is a stepwise process in which XPD acquires its Fe-S cluster before binding TFIIH. This observation suggests that the XPD-CIA targeting complex interaction is required for TFIIH assembly. Fractionation studies indicate that the association of XPD with the CIA targeting complex occurs in the cytoplasm while its association with TFIIH occurs largely in the nucleus where TFIIH functions[50].

According to the most recent study of this year, in mammalian cell lines MMS19 has been also found to interact with POLE1, the catalytic subunit of human Pol ε, except from the iron-sulfur cluster assembly complex CIA protein CIAO1 [51].

The role of DNA polymerase ε has been studied and it has been suggested that it contributes to the replication of both the leading and lagging DNA strands and that Pol has an important role as a proofreading exonuclease in the removal of Pol δ-generated errors from the leading strand. The yeast homolog of Pol ε is Pol2 and it contains an iron-sulfur cluster that is required for DNA polymerase, but not exonuclease, activity [52]. Pol ε has also been found to be involved in DNA repair. According to genetic experiments in budding yeast Pol ε is also implicated in DNA double-strand break (DSB) repair, base-excision repair[53], and S phase cell cycle checkpoint activation. Finally, human Pol ε has been shown to function in nucleotide excision repair in vitro [54].

MMS19 and TFIIH

Previous studies in S.*cerevisiae* has revealed that there is physical association between Hmms19 and two subunits of the TFIIH, which are XPB and XPD[55].

According to studies in S.cerevisiae, the absence of Met18 protein results in slight decrease of protein levels of Rad3 and Ssl2 (XPB) in native conditions. In conditions of stress (growth in poor medium) this effect is more significant. The same study claims that, MMS19 functions in NER by sustaining an adequate cellular concentration of the TFIIH component Rad3 and suggest that Mms19 has distinct and separable functions in NER and cell growth, thus implicating Mms19 protein as a novel multifunctional regulator in cells[44]. The physical association of MMS19 with XPD but not with the other subunits of the TFIIH in mammalian cell lines has been mentioned in two different studies[35][50]. The complex of CIA of MMS19, CIAO1, and MIP18 (FAM96B) is required for the biogenesis of extra mitochondrial Fe-S proteins including XPD. The association of XPD with TFIIH and CIA targeting complex takes place in a mutually exclusive manner meaning that when XPD is associated with the holo-TFIIH is not associated with the MMS19. The appropriate iron levels

and the coordination of FE-S cluster by XPD are essential parameters for the incorporation of the XPD to the holo-TFIIH. According to the same study there is an indispensable peptide docking site for the association of XPD with MMS19 and the further assembly of the first into TFIIH.
The complex in which MMS19, XPD and MIP18 are included is called MMXD and is involved in chromosomes segregation.

At present, any mechanistic understanding of how MMS19 functions in transcription and DNA repair remains elusive. Moreover, the pleiotropic outcomes driven by MMS19 defect are solely addressed to its role in the iron-sulfur metabolism, or the protein has additional functions?

Here, we develop a comprehensive and multidisciplinary approach to dissect the functional contribution of MMS19 in genome maintenance and gene expression regulation.

In order to answer the question about the role of MMS19 Professor Garinis lab has recently generated Mmms19-/- mice; the mice were lethal at an early embryonic stage (Iamartino et al., unpublished results). For this purpose we aim to generate tissue specific knock out animals for MMS19 via the cre/flox system.
The tissue specific MMS19 knock-out animals will be generated by crossing the knock-in mice (MMS19 genomic region (1st exon) flanked by two LoxP sites and a neo cassette (also flanked by to LoxP sites) with transgenic Cre animals that will tissue-specifically drive the expression of the Cre-lox recombinase. The Cre recombinase will drive the excision of the DNA fragment between the loxP sites, so it will lead to the excision of the MMS19 genomic sequence. The first tissue-specific MMS19-depleted animals will be the liver one, by crossing the knock-in animals with the liver specific Cre-transgenic mice, into which the recombinase expression is under control of the albumin promoter.
The development of this new model animal aims to a comprehensive study about the possible phenotypic changes resulted from the depletion of MMS19. Another aspect of the study could be testing the possible transcriptome alterations with micro-array or RNA-seq assay and compare those results with published data, related to other NER defective mice models and or other specific transcription factor defective animals, whose outcomes resembles the one addressed to MMS19 depletion.
It has been difficult to dissect the functional contributions of NER factors in an intact mammalian organism. The budding yeast *Saccharomyces cerevisiae* offers a more versatile and well-developed platform to uncover pathways or screen for direct protein interactions beyond the descriptive level. For this reason in collaboration with Professor Alexandraki's lab we have used the *S. cerevisiae* to dissect the

functional contribution ofMet18 (MMS19) in DNA repair and transcription. For this, we constructed appropriately tagged and gene deleted strains of Met18 protein and examined the effects of exposure to genotoxic stress. We also explored the role of Met18 in transcription indirectly, via studying the effect of its deletion, on Rad3 recruitment to its known targets and the recruitment of Met18protein on the same gene targets. We also examined the effect of Met18 depletion on the expression of Rad3 target genes as well as its effect on Rad3 protein levels.

Materials and Methods

Yeast strains:

FT5

FT5 *met18*Δ (+HYGRO)

FT5 MET18-9MYC (+TRP1)

FT5 RAD3.9MYC (+TRP1)

FT5 *met18*Δ (+HYGRO): FT5 RAD3.9MYC (+TRP1)

FT5 RAD3.3HA (+KANMX6)

FT5 RAD3.3HA:MET18.9MYC (+TRP1)

Media and amino acids used in selection media

Synthetic Complete (SC): 0, 67% bases, 2% glucose, 0, 2% w/v amino acids mix

Yeast extract Peptone Dextrose (YPD): 1% W/V yeast extract, 2% w/v bactopeptone, 2% glucose

Amino acids and drugs used for selection: Leucine 180mM (100X): 2,36% w/v, Histidine 100mM(100X):0,517, Tryptophane 55mM (100X) 1.123% w/v, Uracil 20mM(100X): 0,224% w/v

Zeocin (30µg/ml (Invitrogen)

Kanamycin (200µg/ml, G418, Gibco, Sulphate)

Hygromycin(200µg/ml, Sigma)

4NQO (25µg/ml)

UVsetup

UV irradiation was done on *S. cerevisiae* cells suspended in25ml ddH20 at 200 j/m^2, in a homemade set-up. After the irradiation the cells were centrifuged, and resuspended in 25ml YPD for recovery and activation of the NER pathway for 1h, at 30^{o}C by shaking.

Primers used for tagging and disruption

MET18 tagging for (S3)
5’-GACACAAGACAGGTTTATTATGAATTAGGCCAAATCCCGTTCGAGCGTACGCTGCAGGTCGAC -3’

MET18 disr for (S3)
5’-TGAACTTGTTTTAACTGGGAAAAAGCGGAACAATTGGGCCTTACACGTACGCTGCAGGTCGAC -3’

MET18 disr for (T)
5’-TGAACTTGTTTTAACTGGGAAAAAGCGGAACAATTGGGCCTTACACACTAGCTAAAAAGTGGAAC-3’

MET18 tagging/disr rev (S2)
5’-TTTTCACGTGCTCATCAATGTGAACAAATTATTAAATACAAGCGTATCGATGAATTCGAGCTCG-3’

RAD3 tagging for (S3)
5’-GAAGGAGAACAGGATGAAGATGAAGATGAAGATATAGAAATGCAGCGTACGCTGCAGGTCGAC-3’

RAD3 tagging rev (S2)
5’-TCTAATTGTGATATATACAGTTTATAGCAAAAGCGTATCATTGCAATCGATGAATTCGAGCTCG -3’

Plasmids used for tagging and disruption

PYM1-> tagging with 3HA (with kanamycin resistance as selection marker)

Pym6 -> tagging with 9Myc (with tryptophan auxotroph as selection marker)

Pag32 -> disruption of Met18 (with hygromycin resistance as selection marker)

Bacterial competent cells: DH5a

Bacterialtransformationwithheat shock

The already made competent cells are incubated from -80^{o}C in the ice for 8-10min. After the addition of the plasmid DNA to the competent cells they are incubated for 20min on ice. Then they are transferred to 42C for 1min. Then the bacterial cells are left to recover in LB for 1h at 37^{o}C. Finally, the cells are platted on solid LB with antibiotic (as marker/ampicillin) and incubated overnight at 37^{o}C.

Plasmid DNA extraction by Mini prep Kit->Qiagen prep Spin

HIGH EFFICIENCY YEAST TRANSFORMATION

Day 1

Inoculation of the yeast strain into 5 ml of liquid medium (2xYPD or SC selection medium) and incubation overnight on a rotary shaker at 200 rpm and 30°C

Day 2

1. Determination of the titer of the yeast culture by a spectrophotometer cuvette and measure the OD at 600nm. For many yeast strains a suspension containing 1x10^{6} cells/ml will give an OD_{600} of 0,1.

Dilution of the overnight YPD or SC cultures in 20ml YPD or SC in a flask on a rotary or reciprocating shaker at 30°C and 200rpm takes place. It is important to allow the cells to complete at least two divisions. (This will take 3 to 5 hours.) Transformation efficiency (transformants/μg plasmid DNA/10^8 cells) remains constant for 3 to 4 cell divisions.

When the cell titer is at least 1x10^7cells/ml, which should take about 4 hours, the cells are harvested by centrifugation at 3000rpm for 3min, 4^{o}C. They are washed in 20ml of sterile water (2min, 3.000rpm, 4^{o}C) and resuspended in 1ml of LiAc 0,1M. The cell suspension is transferred to a 1,5ml Epp. Tube and it is centrifuged for 1min, 13.000rpm. After discarding S/N the pellet is resuspened in 200λ LiAc 0,1M and re-centrifuged for 30sec

Boiling of a 1ml sample of carrier DNA takes place for 5min and chilling in an ice/water bath while harvesting the cells.

Sufficient Transformation Mix (PEG 50% w/v, LiAc 1M, Boiled SS-carrier DNA, PCR product DNA, ddH20 is prepared and it is kept on ice.

The transformation Mix is added to each transformation tube and the cells are resuspended by vigorous vortex and they are incubated in 30^{o}C for 25min, and in a 42°C water bath for 30 min.

The following step is the plating of appropriate dilutions of the cell suspension onto SC selection medium. For transformation with an integrating plasmid (YIp), linear construct or oligonucleotide, plate 200λ onto each plate. In SC plates appropriate amino acids are added according to the auxotrophies used for selection markers of the transformation.

Note: Incubation of the plates at 30°C for 3 to 4 days takes place and then counting of the number of transformants in order to measure the transformation efficiency (transformants/1μg plasmid DNA/10^8 cells) can be determined by calculating the number of transformants in 1ml of resuspended cells per 1μg plasmid per 10^8 cells.

Genomic DNA extraction

The colonies that are used for genotyping about the tagging or the disruption of the *MET18* and *RAD3* genes are inoculated into liquid medium (2xYPD or SC selection medium) and they are incubated overnight on a rotary shaker at 200rpm and 30°C. The next morning the cultures are transferred to Eppendorf tubes. After centrifugation the cells are washed with ddH20. Then mechanical lysis of the cells takes place by incubating them with equal volumes of breaking buffer, glass beads, phenol chloroform and ddH20. After centrifugation the pellet is resuspended in absolute ethanol are centrifuged again. Then the pellets are resuspended in ddH20

and treated with RNase (10μg/λ), 30min-1h, 37°C. The precipitation of DNA takes place by incubating the samples with NH4Ac 4M and absolute ethanol for 20min in -20°C. The salts are eliminated by 70% ethanol and after centrifugation the samples are finally resuspended in ddH20 (35-50λ).

Primers used for checking tagging and disruption of

Sequence (5'->3')	Length	Start	Stop
Met18-400FTTTTCCTGTGTGGCTGTCGTT	21	-400	
MET18+2701FAGCCAATCGGTTGGTCCTTT	20	2701	2720
MET18+2999RGCGCTTAGAACATCGTCCTG	20	2999	2980
RAD3+1896F GCGTATTTTGAAAGCTCGCCT	21	1896	1916

KAN&HIS primer: TGGGCCTCCATGTCGCTGG

TRP primer: GCTATTCATCCAGCAGGCCTC

Chromatin ImmunoPrecipitation from yeast whole cell extracts (ChIP from WCE)

STARTER CULTURE

A small amount of the specific strain used during the experimental procedure is inoculated in 3ml YPD media and it is incubated O/N, 30°C, shaking. The next day the starter culture is diluted to OD~0.25 (50-100ml YPD/~50-100 ODs). When the OD reaches 1-1,5 the appropriate treatment is done (eg. 4NQO or UV). After treatment the diluted culture is incubated for 1h, 30°C, shaking in order to recovery from the stress, that has faced, during the treatment. The OD after the recovery should be 1-1,5.

CROSS-LINKING

The cells are treated with 1% formaldehyde, shaking, RT for 20min, in order to fix the DNA-protein interactions and the protein-protein interactions that take place. The neutralization of formaldehyde activity is achieved by incubating the cells with glycine 2.5M, 5min, RT, shaking .Then washing of the cells with ice cold TBS takes place. (Centrifugation 3min, 2.500rpm, 4°C, Discard S/N and resuspend the pellet in 15-20ml TBS (COLD) and shake well X2. After washing the cells can be kept as a pellet in -80°C or proceed to the lysis step.

CELLS LYSIS

Each cell pellet is washed and resuspended in TBS buffer. The resuspension is transferred in 2ml tubes. After Centrifugation 2min, 13.000rpm, the pellet is resuspended in lysis buffer (FA/ISO) with PIC (3% SIGMA stock) and PMSF (1:100) (100mM stock). PIC and PMSF are proteinase inhibitors that eliminate their activity, in order to keep intact the DNA-protein interactions and the protein-protein interactions that take place. Mechanical cell lysis is achieved by vortexing the cells with washed glass beads (cold/ prechilled) for 1h in the cold room (4^{o}C). After the mechanical cell lysis, the Eppendorf tubes are transferred in 15ml falcon (sterile) and centrifuged for 4min, 2.000rpm, 4^{o}C. A hole to the Eppendorf tubes is done with burnt needle and the cells extracts are transferred in new 2ml Eppendorf tubes (cells+ S/N)

SONICATION

The sonication of the chromatin of the cell extracts takes place via manual sonication. (10X*80% amplitude, 45sec (ON ICE with sterile probe).

* Depends on the samples and the preferable length of the DNA (~300-400bp).After sonication, the samples are centrifuged for 20min, 13.000rpm, 4^{o}C X2 and the S/N is transferred in new cold Eppendorf tubes

IMMUNOPRECIPITATION (IP)

1/10 of the sonicated sample is kept as INPUTs (5-10ODs). The rest of the samples are incubated with 50λ pre-equilibrated beads into lysis buffer (conjugated with the antibody/Easy view red anti-cmyc affinity gel/Sigma) with 5λ PIC (Proteases inhibitors cocktail) and PMSF (1:100), O/N on rotating carousel, in the cold room (4^{o}C).

The equilibration of the beads is done according to the following procedure:

Add 50λ in each tube add 1ml Lysis buffer mix gently by inversion

Centrifuge 8.000rpm, 1min, RT and discard S/N (CAREFULLY) without interrupting the beads X2

The next morning the beads washing takes place. The IP samples are centrifuged 1min, 8.000rpm and S/N is discarded or kept as F/T. The pellet is re-suspended in 1ml Lysis buffer (FA ISO) + 10λ PMSF (100mM) and incubated on rotating carousel, 5min X2.Then the samples are centrifuged 1min, 8.000rpm and the S/N is discarded. The pellet is resuspended in 1ml Lysis buffer (FA ISO 500) +10λ PMSF (100mM), and incubated on rotating carousel, 5min X3. After centrifugation 1min, 8.000 rpm, S/N is

discarded. The pellet is resuspended in 1ml Wash III buffer without PMSF (100mM) and incubated on rotating carousel, 5min X2. After centrifuge 1min, 8.000rpm the S/N is discarded and the pellet is resuspended in 1ml TE buffer without PMSF (100mM) and incubated on rotating carousel, 5min X2. The washed beads are further centrifuged 1min, 8.000 rpm and S/N is discarded. The RNase treatment takes place by incubating the beads, with 100λ TE+2,5λ RNase (10γ/λ) for 30min-1h, 37^{o}C. (The same is done for INPUTS). ChIP elution buffer is added ONLY TO INPUTS up to 500λ volume and they are kept on ice.

Elution of DNA from the beads

The next step is the elution of DNA from the beads. During this process 1ml TE is added in the IP samples. They are shacked gently, centrifuged 1min, 8.000rpm, resuspended in 250λ elution buffer, incubated on rotating carousel for 5min and vortexed for 30sec X3. After centrifugation 1min, 8.000rpm, the S/N is transferred in new cold Eppendorf tubes and the previous Eppendorf tubes are treated with 250λ TE. The same procedure that took place in the first Eppendorf tubes is repeated in the second meaning that they are incubated on rotating carousel for 5min vortex for 30sec X3. They are centrifuged 1min, 8.000rpm and the S/N is transferred in the exact tubes (Pool the extracts). Both the IPs and the INPUTs are treated with 40λ 2,5M NaCl and incubated O/N at 65^{o}C (de-crosslinking takes place).

The next day the precipitation of the chromatin takes place by incubating both IPS and INPUTS samples with 1ml 100% ETOH, in -80^{o}C O/N or for at least 2h.

The next morning proteinase treatment DNA extraction takes place. Firstly the samples are centrifuged for 20min, 13.000rpm, 4^{o}C, S/N is discarded and 70% ETOL is added in the pellet. Further centrifugation for 3min, 13.000rpm, 4^{o}C takes place. The S/N is discarded and the samples are dried in the Speedvac and the pellet is resuspended in 200λ TE. The samples are treated with 10xlysis buffer and Proteinase K (20γ/λ) and incubated at 50^{o}C for 30min.The DNA extraction is done by the phenol/chloroform method.

The samples are treated with 200λ Phe/chl and centrifuged 3min, 13.000rpm, 4^{o}C. The S/N is transferred in new Eppendorf tubes. Back-extraction is done by adding 200λ Phe/chl in the previous Eppendorf tubes. Centrifugation is done for 5min, 13.000rpm and the S/N are transferred in the exact tubes (Pool the extracts). 400λ Phe/ch is added in the pooled extracts. The pooled extracts are centrifuged 3min, 13.000rpm and the S/N is transferred in new Eppendorf tubes. The samples are further treated with 400λ chloroform and centrifuged 3min, 13.000rpm. The S/N is transferred in new Eppendorf tubes and treated with 40λ CH3COONA (1:10), glycogen (40γ/λ) and 2,5V absolute ETOL and incubated in -80^{o}C O/N or for at least 2h. Then the samples are centrifuged 30min, 13.000rpm, 4^{o}C and S/N is discarded.

The precipitation of DNA takes place via 500λ 70% ETOl. Then further centrifugation is done for 3min, 13.000rpm and S/N is discarded. DNA is dried in the Speedvac for 5min, 45^{o}C. The pellet is resuspended in the appropriate volume of ddH20 (depending on the OD of each sample). After resuspension RT-PCR can be done.

Primers used for Q-PCR

Name Forward primer Reverse primer

PROM *ADH1*
ADH1-1
ATAGGCGCATGCAACTTCTT CATCAGCTCTGGAACAACGA
PROM *ADH1*
ADH1-2
TTCCTTCATTCACGCACACT AGGGAACGAGAACAATGACG
ORF *ADH1*
ADH1-3
GGGTATTGACGGTGGTGAAG AAACGTTGATGACACCGTGA
ORF *ADH1*
ADH1-4
GGCTGGAAGATCGGTGACTA TCAGCGGTAGCGTATTGTTG
ORF *ADH1*
ADH1-5
GGTGCCAAGTGTTGTTCTGA GACAAGCCGACAACCTTGAT
PROM *PYK1*
PYK1-1
CGCACCGTCACAAAGTGTTTGGGAAGGAAAGGAAATCAC
PROM *PYK1*
PYK1-2
CCTTTCCTTCCCATATGATGCACTTTGAAAGGGGACCATGA
ORF *PYK1*
PYK1-3
TGCTTTGAGAAAGGCTGGTTTCTGATTTCTGGACCCTTGG
ORF *PYK1*
PYK1-4
ATGGTTGCCAGAGGTGACTT TCTGGTTGGTCTTGGGTTGT
ORF *PYK1*
PYK1-5
CAGAGGTGTCTTCCCATTCG CCTTGAAACCTTGGATGGAA

ORF *GAL1*

AAAGAAACTTGCACCGGAAA GGCCCATATTCGCTTTAACA

RNA extraction

The appropriate yeast strains are inoculated in 3ml YPD and overnight incubation at 30^{o}C, shaking takes place (starter culture).

The next morning the starter culture is diluted and incubated in YPD, at 30^{o}C shaking, until the cells number is 10^{8}.Then the cells are washed in ddH20 and resuspended in AE buffer (Sodium acetate 3M, EDTA 0,5M) for cell lysis. 1/10 volume SDS is added and equal volume of phenol.

Then the samples are transferred at 65^{o}C for 5min, then in dry ice with ethanol for 5min and again at 65^{o}C for 5min. After their incubation at 65^{o}C, for 4min and centrifugation the upper phase is transferred in a new Eppendorf tube and treated with equal volume of phenol/chloroform. After centrifugation the upper phase is transferred in a new Eppendorf tube and is treated with equal volume of chloroform. After centrifugation the upper phase is transferred in a new Eppendorf tube and RNA precipitation takes place via incubation of the sample with 70% ethanol, at -80^{o}C overnight.

DNase Treatment

5μg of RNA samples are treated with 2units DNase in DNase buffer and are incubated for 1h at 37^{o}C.

Then the samples are treated with 1/10 volume sodium acetate and phenol chloroform extraction takes place as described in the RNA extraction procedure.

Reverse transcription

The reverse transcription takes place in order to produce cDNA from the RNA samples. 1,5μg of RNA is treated with two different mixes. Mix1: random primers (60μM, 10mM dNTPs) incubation 5min, 65^{o}C. Mix2: 40units/λ Reverse transcriptase, Reverse transcriptase buffer (5X), 0, 1M DTT, RNase inhibitor.

Incubation temperatures: 10min -> 25^{o}C, 50min -> 42^{o}C, and 20min -> 65^{o}C

Protein extraction from *S.cerevisiae*

The optical density of the appropriate yeast cultures is measured and specific amount of culture is transferred to an Eppendorf tube in order to the final concentration to be 10ODs. Then this amount of cells is washed with ddH20 and resuspended in 0,2M NaOH for cell lysis. After the cell lysis the extracts are boiled in 100C with Protein loading buffer (60mM Tis-HCL pH 6, 8,5% glycerol, 2% SDS, 4% mercaptoethanol and 0,02% bromothenol blue). After centrifugation the protein

extracts are either kept in -80°C or loaded in a polyacrylamide SDS page gel for Western blot analysis.

Western blot

Gel preparation: The stacking and separating (8% and 10%) gels were prepared according to the standard protocols. For Loading: 5-10 ODs of protein were loaded in case of inputs. Running: 150volt 1h, RT. Transfer: 220mA, 2h, 4°C or overnight, Blocking: 5%milk, 1h rocking plate, RT. Antibodies: Rabbit SC 789 anti-Myc, Rabbit CST 37245 anti HA.

The targeting vector for MMS19 floxed/floxed gene in <u>mouse</u> embryonic stem cells JM8

The first step in order to develop the MMS19fl/fl is to insert a targeting vector containing MMS19 genomic region (1st exon) flanked by two LoxP sites and a neomycin resistance cassette (also flanked by two LoxP sites) in mouse ES cells (**JM8**) cells via electoroporation (**Figure 6**). The JM8 cell line are embryonic stem cells derived from C57BL/6 strain mouse. After electroporation, when homologous recombination occurs the genomic region should be replaced by the targeting vector containing the genomic region of MMS19 flanked by LoxP sites. After the insertion of the targeting vector the transformed cells will be resistant to Neomycin.

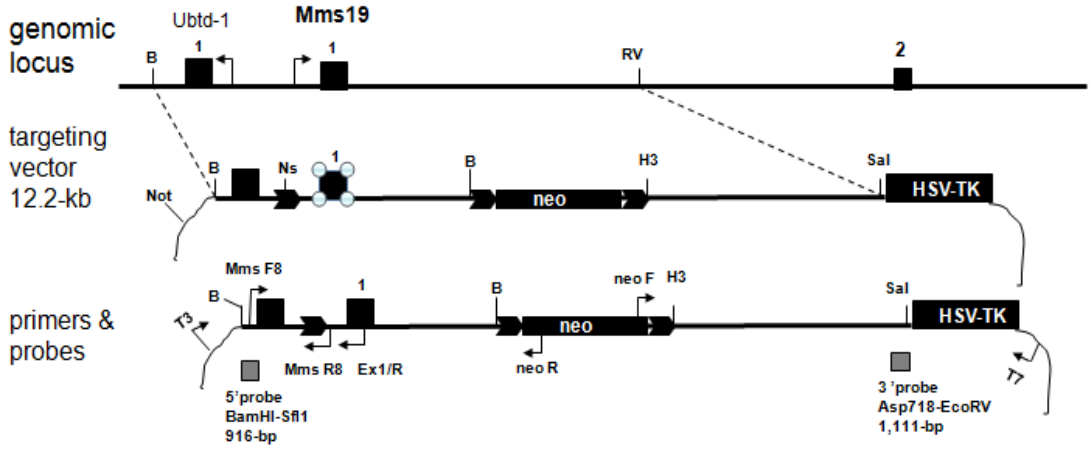

Figure 6: The genomic sequence of MMS19 is illustrated. The two first exons of the locus are symbolized with 1 and 2. Ubtd1 is the gene located before Mms19 gene locus. The arrows indicate the direction of transcription. The targeting vector used during the electroporation is illustrated. The letters symbolize the restriction sites of the vectors (B: BamHI, H3: HindIII, Sal1 and Not1). The primers and probes used for checking the appropriate integration are described (5' probe isolation: BamHI-Sfil 916-bp and 3' probe isolation: Asp 718-EcoRV 1.111bp).

ELECTROPORATION OF JM8 cells:

Day 1 : Thaw 1 vial of JM8 clone early in the morning onto a 6cm plate with Complete medium: (82% DMEM , 15% FBS, 1,5 PSG, 1% Non-Essential Amino acids, 0,0007% Mercaptoethanol, 0,2% hLIF) containing mitogenic inhibitors (mitogen-activated protein (MAP) kinase inhibitor and glycogen synthase kinase 3 (GSK3) inhibitor).

Day2: Changing the complete medium. Closely monitoring of the morphology as it is vital that cells are in the optimum condition. (Differentiation is observed as loss of discreet JM8 cell colony border, the formation of cobblestone-like cells and stretched fibroblasts extending outward of the colony. Undifferentiated cells grow in small, smooth, round aggregates).

Day3: Changing of the medium in the morning. Cells must be 70-80% confluent around noon. One to two hours after the medium change, pass cells to 2x10cm plates.

Day4: Changing of the media and monitor the cells (should be confluent the next day…). Chose to expand the cells, splitting into additional 10cm plates, according on the amount of cells scheduled for the electroporation.

Day 5: Changing medium of the cells 2-4 hours prior to electroporation and washing cells with 10ml 1XPBS, trypsinization is done with 0,3% Trypsin. The cells pellet is isolated by centrifugation at 1000rpm, 5min.The supernatant is aspirated and the pellet is resuspended in 1XPBS for electroporation

The cell density is determined by using a hemocytometer.

For each electroporation: mix together 25-30λ of 15-40µg DNA (approximately 1µg/λ DNA per 0.9ml of 1XPBS ($1,1X10^7$ CELLS/0,9ml 1XPBS).The cell suspension is transferred to 0.4cm electroporation cuvette and incubated at RT, 5min.

The cuvette is placed in the electroporator (Pulse the cells once at 230Volts and 500µF Capacitance (The time constant [RC] should be 6,9-7,2 (7,2 optimum)

The cell suspension is transferred from the cuvette to a sterile tube containing pre-warmed media and distribute equally onto 10cm feeder dishes containing 10ml warmed normal medium. (Recovery after electroporation).

After electroporation the cells are cultured with the selection media containing the Neomycin (ES media+200µg/ml of Neomycin) onto 10cm feeder dishes. The clones that have survived after the selection are transferred, under low power magnification of stereoscopic microscope in pregelatinised-96-well-plates in normal ES media. Then these clones are trypsinized (0,3% trypsin) and further transferred in

24 well-plates. When the confluency of the cells is 70-80%, they are separated in two aliquots. The one aliquot is transferred in cryovials containing freezing media (medium+10% DMSO). Genomic DNA is extracted via phenol/chloroform protocol from the other aliquot, and it is used as a template in PCR reactions in order to check the appropriate integration of the LoxP sites in the genomic locus of interest/MMS19, via homologous recombination and not in unspecific region.

The homologous recombination is further checked via Southern blots, with radiolabeled probes corresponding to the genomic sequence of MMS19. The radiolabeling of probes (5' probe isolation: BamHI-Sfil 916-bp and 3' probe isolation: Asp 718-EcoRV 1,111bp) takes place via the random priming method. This method is based on the 5'-3' exonuclease activity of the Klenow Polymerase. The protocol used was the *prime-a gene labeling system* (Promega).The reagents used during the radiolabeling are: 5xklenow polymerase buffer, dNTPs, BSA, dCTPs (radioactive nucleotides in radioactive Ph), Klenow polymerase. The DNA template was isolated by gel extraction kit (QIAquick Gel Extraction Kit, Qiagen)

The radiolabeled probes are cleaned in pre-equilibrated columns. (Columns are made by 1ml Syringes with sephadex and are treated with G50. The pre equilibration of the columns is done with 100λ TNE, Spin and 5min, 1.200rpm)

50λ probe, 150λ Salmon Sperm DNA, 50λ TE are centrifuged in the columns for 5min, 1200 rpm. They are annealed at 100^{o}C for 5min and immediately incubated with the membranes, 65^{o}C, O/N. The annealing of the probes results in single stranded radiolabeled DNA, which is able to hybridize with the genomic DNA, which is transferred on the nylon membranes used for the Southern blotting.

Results

Epitope-tagged Met18 (Met18.9myc) strain was constructed in S.*cerevisiae*

The first step for examining the role of Met18 in transcription and repair was to study the possible targets of Met18. Epitope tagging was used in order to develop tagged versions of the Met18 protein that allow the detection of Met18 protein. The tagged version is Met18.9myc in WT S.*cerevisiae* strain (FT5). During epitope tagging the production of a linear PCR product containing the sequence of the gene with the sequence of the tag at the carboxyterminal end of the protein takes place Figure 7a. Then this product is inserted in the yeast genome via yeast transformation assays. The verification of the epitope tagging was done both in the DNA and in the protein level by PCR and Western blot respectively **Figure 7a and 7b**. The epitope tagging was successful in 3, 4, 5 clones.

a) b)

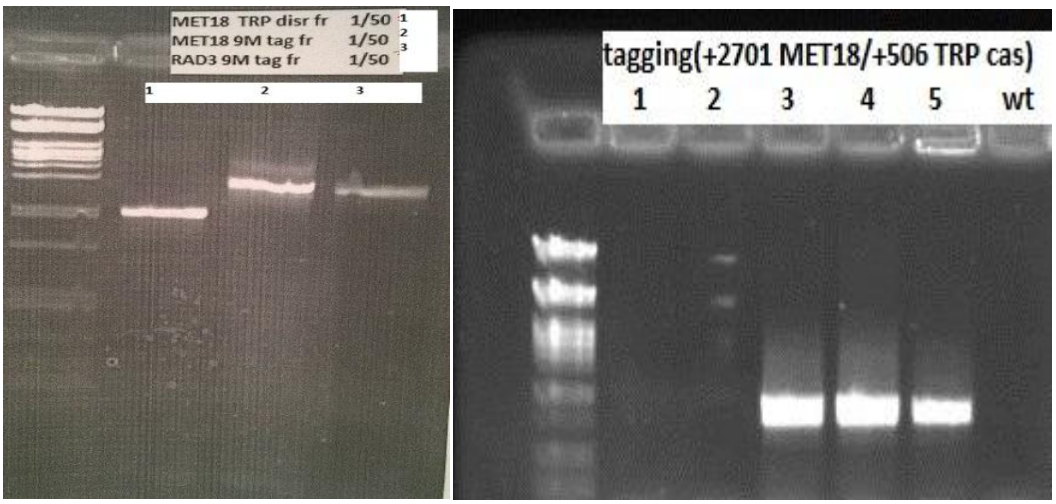

c) d)

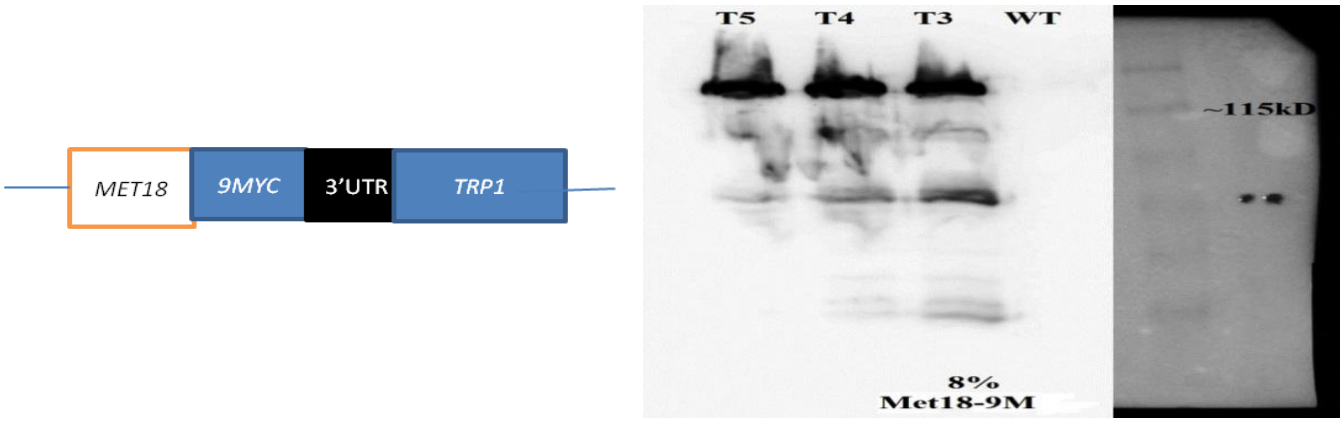

Figure 7: a) In the first 1,5% agarose gel 1λ of the PCR products used for Met18 tagging and disruption are presented. b) In the second gel the verification of Met18 tagging was done by PCR with primers specific for the sequence of Met18 and for the sequence of the selection

marker corresponding to the sequence of the tag 9 Myc. c) The construct of linear PCR product used for transformation containing the ORF of Met18, 9Myc tag, 3'UTR and Tryptophane auxotrophy selection marker is presented. d) Western blot checking the expression of the tag with negative control a WT (untagged) strain is presented on a 8% polyacrylamide gel. The protein marker is also illustrated. The molecular weight of the protein with the tag is 115kD as mentioned in the nitrocellulose membrane presented. The image was taken by the Las-3000 (Fujifilm) and the exposure after the ECL treatment was 4min.

Met18 protein was not recruited to Rad3 target promoters in both native and DNA damaging conditions

In order to find out Met18.9Myc possible targets ChIP-RT experiments took place. Since its localization on these targets are completely unknown and the physical interaction of Met18 with Rad3 is known[46], it was examined whether Met18 binds to the known targets of Rad3[56] in native conditions (YPD) and in conditions of damage. In order to induce the damage and the activation of the NER pathway we treated the cells with 4NQO (mimetic drug of UV). It can be concluded according to the plot presented in Figure 8 that Met18 did not bind to the promoters of the targets of Rad3 in both native conditions and in conditions of damage since the binding of Met18 in the examined genes is not significantly higher compared to the binding at the negative control which is *GAL1*.

The experiment about the binding of Met18 at the promoters of one of the targets of Rad3 was repeated using as positive control Rad3.9myc strain. The construction of Rad3.9myc strain was achieved by the same methodology used for the construction of Met18.9Myc.Epitoppe tagging was checked both at the DNA and at the protein level by PCR and Western blot respectively **Figure 9b and Figure 9d**. As illustrated in **Figure 9b** the epitope tagging was successful in 6 clones (1-6).

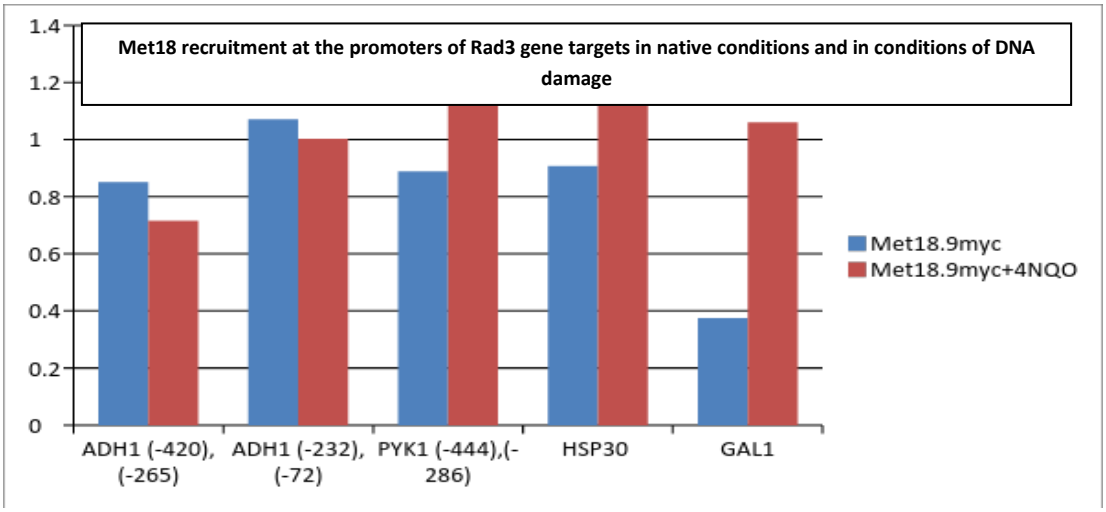

Figure 8: ChIP-RT experiment results are exhibited about Met18 possible bindings to the known targets of Rad3 in native conditions (YPD).The strain used was Met18.9Myc illustrated with the blue bars. DNA damage and the activation of the NER pathway were induced by treating the cells with 4NQO (mimetic drug of UV) illustrated with the red bars. The genes examined are *ADH1, PYK1, HSP30* and *GAL1* and the numbers in the plot indicate the region of the promoter examined during the RT-PCR. *GAL1* was used as a negative control.

a)

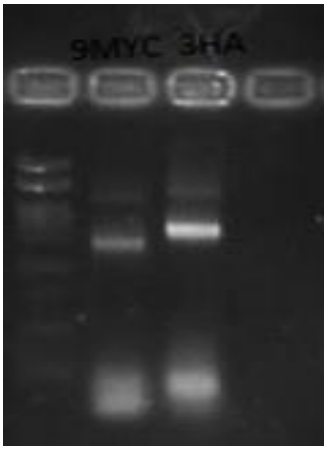

b)

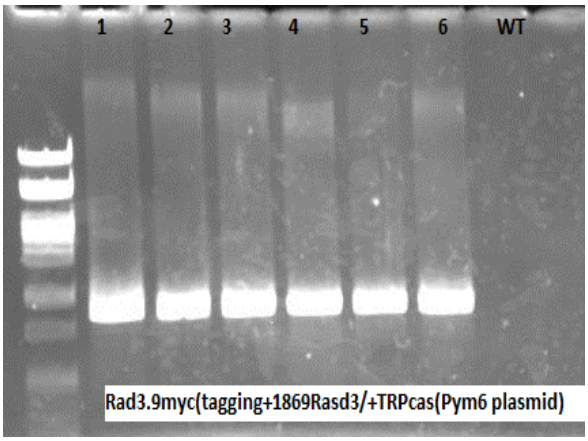

c)

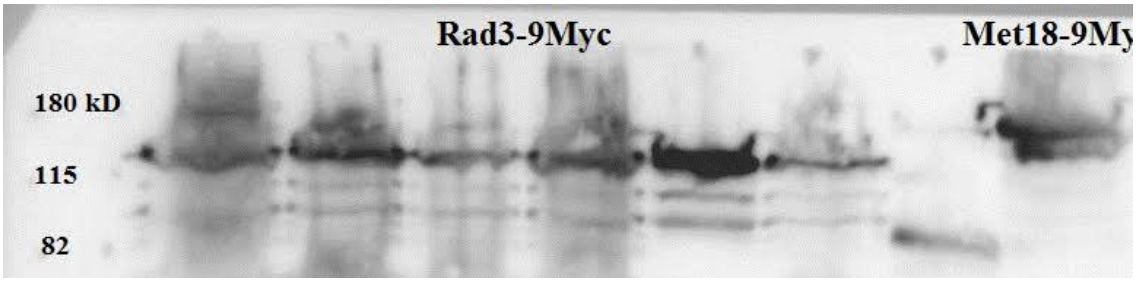

d)

Figure 9: a) In the first 1,5% agarose gel 1λ of the PCR products used for Rad3 tagging are presented. b) In the second gel the verification of Rad3 tagging was done by PCR with primers specific for the sequence of Rad3 and for the sequence of the selection marker corresponding to the sequence of the tag 9 Myc. The construct of linear PCR product used for transformation containing the ORF of Rad3, 9myc tag, 3'UTR and TRP auxotrophy selection marker is presented. d) Western blot checking the expression of the tag with negative control a WT (untagged) strain is presented in a 10% polyacrylamide gel. The molecular weight of the protein with the tag is in between 115kD and 180kd as indicated according to the protein marker, in the nitrocellulose membrane presented. The image was taken by the Las3000 (Fujifilm) and the exposure after the ECL treatment was 2min.

It was also examined whether Met18 possible binding was affected at different DNA damage conditions. We treated the cells with Zeocin (1h recovery, 30μg/ml in YPD) or with 200j/m^2 (UV irradiation was done in cells suspended in25ml ddH20) and

rested for recovery and activation of the NER pathway for 1h at 30°C, by shaking in YPD. Following recovery the cells were further processed for crosslinking and kept at-80°C for the ChIP experiment. It seems that Met18 did not bind to *PYK1*promoter (target of Rad3) under both native and damaging conditions since the binding of Met18 on the examined genes was not significantly higher compared to the binding at the negative control which is *GAL1* promoter(**Figure 10**).

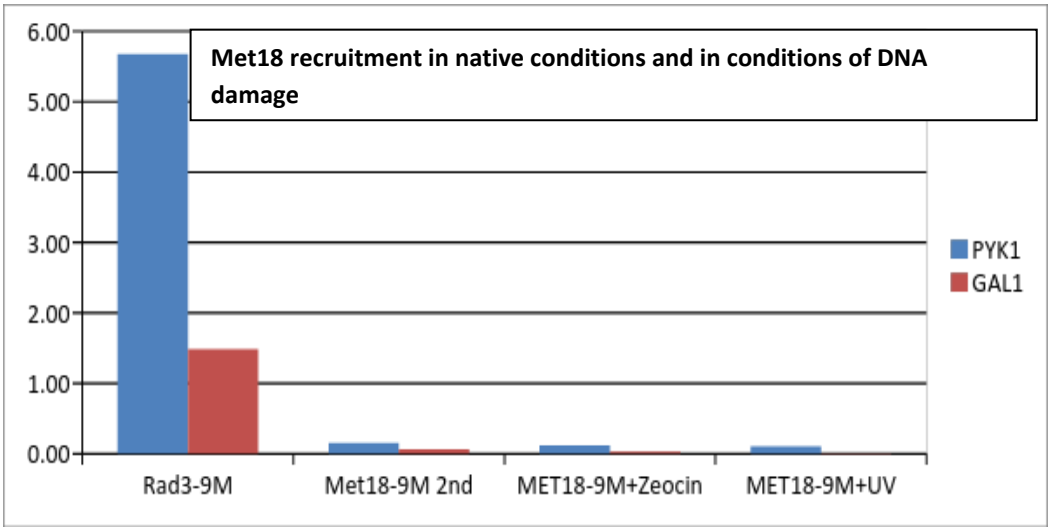

Figure 10: ChIP-RT experiment results are exhibited about Met18 possible bindings to the known targets of Rad3 in native conditions (YPD) and in conditions of DNA damage. The strains used were Met18.9Myc and Rad3.9Myc as a positive control. The genes examined are *PYK1*(blue bars) and *GAL1* (red bars). *GAL1* was used as a negative control. DNA damage and the activation of the NER pathway were induced by treating the cells Zeocin (1h recovery, 30μg/ml in YPD) or with 200j/m^2 (UV irradiation was done in cells suspended in25ml ddH20) and rested for recovery and activation of the NER pathway for 1h, 30°C, Shaking.

Met18 depletion and genotoxic stress resulted in decreased recruitment of Rad3 to its target genes

We wanted to further asses the role of Met18 on the recruitment of Rad3 to the promoters of its known targets. For this purpose we used the strain with disrupted the expression of Met18 (*MET18* deletion) and the tagged version of Rad3 (*met18*Δ.Rad3.9Myc). We used as control the WT strain (Rad3.9myc) and we treated the cells with UV irradiation or Zeocin (the same dosage and time used in the previous experiment). The construction of the strain *met18*Δ.Rad3.9 Myc was done in two steps (**Figure 11**). Firstly, the deletion of *MET18*ORF from yeast genome took place by yeast transformation with a linear PCR product containing *MET18*ORF flanking sequences and a selection marker (Hygromycin resistance gene) for the replacement of *MET18* ORF. The verification of *MET18* deletion following yeast transformation, homologous recombination event and survival in the presence of Hygromycin was done by PCR with primers specific for the ORF and for the selection

marker (Figure 11a). In this strain (*met18*Δ) epitope tagging also took place and was also verified by the same methodology used for the verification of Rad3.9myc epitope tagging in the WT strain (FT5) **Figure 11b and figure 11**.

a) b)

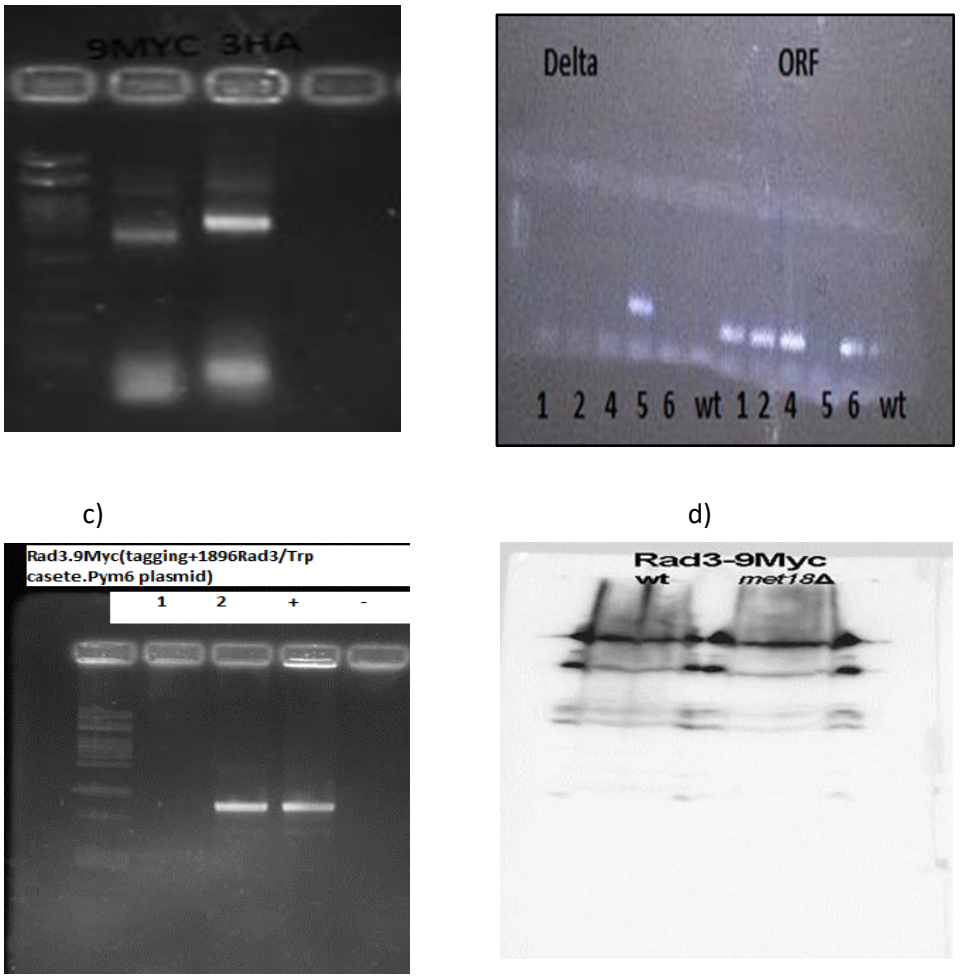

Figure 11: In the first 1,5% agarose gel 1λ of the PCR products used for Rad3 tagging are presented. The verification of *MET18*ORFdeletion was checked by PCR reaction checking the presence of the Hygromycin resistance marker, which is part of the plasmid used for the deletion of *MET18*ORF. In the same gel the absence of *MET18* ORF was also examined. The 5th clone is the clone exhibiting*MET18*ORFdeletion and the presence of Hygromycin resistance gene sequence. This clone was used for further transformation with the Rad3.9myc tagging fragment which is illustrated in fig.11 b). c) The verification of the Rad3.9myc tagging in *met18*Δ strain was done with PCR. As positive control genomic DNA from Rad3.9myc strain was used. As negative control genomic DNA from a WT strain (FT5: untagged) was used. Clone 2 is positive for the presence of Rad3.9Myc tagged. dThe verification of the appropriate expression of Rad3.9myc in the*met18*Δ strain was done with Western blot and antiMyc. As positive control Rad3.9Myc strain was used. *met18*Δ strain contains in its DNA and expresses tagged version of Rad3 (Rad3.9myc) protein.

We performed ChIP experiments in the aforementioned strains (*met18*ΔRad3.9Mycand Rad3.9myc) in native conditions (YPD) and in conditions of DNA damage (Zeocin and UV irradiation). More specifically, we treated the cells with Zeocin (1h recovery, 30μg/ml in YPD) or with 200j/m^2 (UV irradiation was done in cells suspended in25ml ddH20) and rested for recovery and activation of the NER pathway for 1h, 30°C, shaking. Following recovery, the cells were further processed for crosslinking and kept at -80°C for the ChIP experiment.

According to the plot presented in **Figure 12**, genotoxic stress affected the recruitment of Rad3 to its targets in the WT strain. More specifically, the cells treated with zeocin or UV exhibit less recruitment of Rad3 to its targets. The effect of Zeocin to the recruitment at *PYK1* promoter seems to be more severe compared to the effect of UV. As far as, Rad3 recruitment to *ADH1*, it is dramatically decreased but the effect of UV and Zeocin are almost equal. Also according to the same plot, there is a decrease in Rad3 recruitment upon genotoxic stress also in the *met18*Δ strain. In this case, UV seems to have more severe effect on Rad3 recruitment both at *PYK1* and *ADH1* promoters.

By comparing the two strains, we can conclude that, when Met18 is missing (*met18*Δ) Rad3 recruitment to the targets was decreased compared to WT. The levels of Rad3 binding also seemed to be affected by the damaging conditions both in the WT and in the deletant (*met18*Δ). The effect of UV is tremendous in the mutant strain, while the effect of zeocin seems to be more severe in the WT strain. So we can conclude that both Met18 depletion and DNA damage affect the localization of Rad3 but their effect seems to act synergistically, meaning that UV treatment has stronger effect when Met18 is absent.

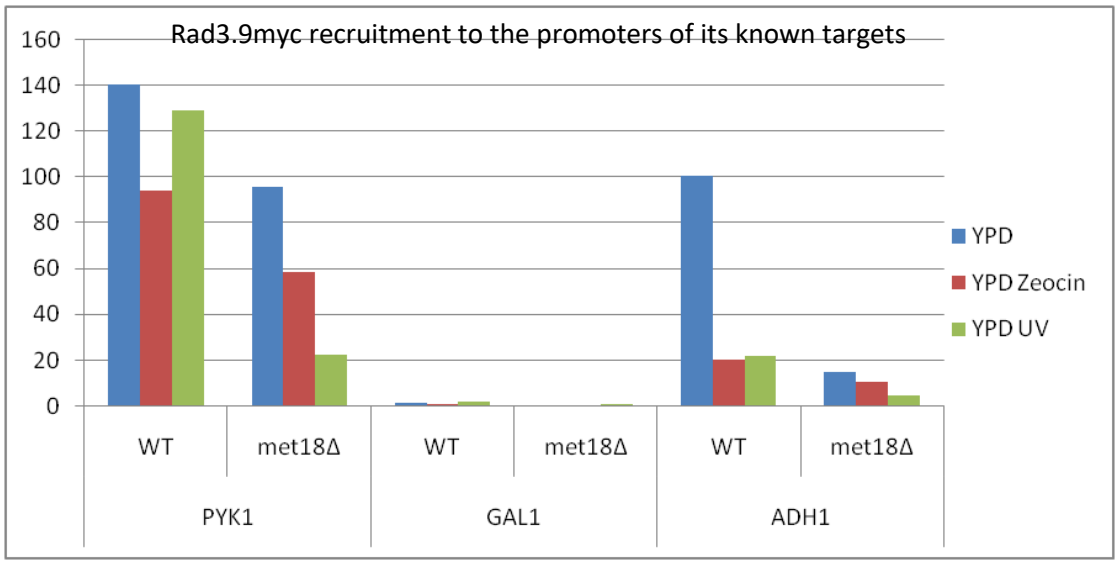

Figure12: ChIP-RT experiment took place in order to examine the role of Met18 to the Rad3 recruitment in native conditions (YPD) and in conditions of DNA damage. WT strain (Rad3.9myc) was used for ChIP-qPCR experiment. The strain with disrupted the expression of Met18 and tagged version of Rad3 (met18Delta.Rad3.9 Myc) was used for ChIP-qPCR experiments. The genes examined are *PYK1* and *GAL1. GAL1* was used as a negative control. DNA damage and the activation of the NER pathway were induced by treating the cells with Zeocin (1h recovery, 30μg/ml in YPD) or with 200j/m^2 UV irradiation (UV irradiation was done in cells suspended in25ml ddH20) and rested for recovery and activation of the NER pathway for 1h, 30^{o}C, Shaking. After the resting the cells were further processed for crosslinking and kept at -80C for the ChIP experiment.

Met18 disruption decreased Rad3 protein levels whereas UV irradiation did not affect them

To further understand the above results we examined whether the levels of Rad3 protein were affected when *MET18*was deleted and under conditions of DNA damage. The effect of met18 depletion on Rad3 protein levels has been examined in another study in native conditions but the effect of UV irradiation had not been studied before. For this purpose, cells from WT (Rad3.9Myc) and *met18*Δ (*met18*ΔRad3.9myc) strain were treated with UV irradiation (200j/m^2 UV irradiation was done in cells suspended in25ml ddH20/same treatment as in ChIP experiments).From these cells protein extraction and WB with anti-Myc were performed.

Another question addressed, was which could be the effect of UV irradiation in the stability of Rad3 protein. More specifically, the possible change of Rad3 protein levels, during different time points post UV irradiation were examined. For this purpose after UV treatment (200j/m^2 UV irradiation was done in cells suspended in25ml ddH20/same treatment as in ChIP experiments) cells from WT (Rad3.9Myc) and *met18*Δ (*met18*ΔRad3.9myc) strains were treated with UV irradiation and they were incubated at 30^{o}C for 15min, 30 min, 60min and 120min. 10^{7} cells from each time point were used for protein extraction and western blotting.

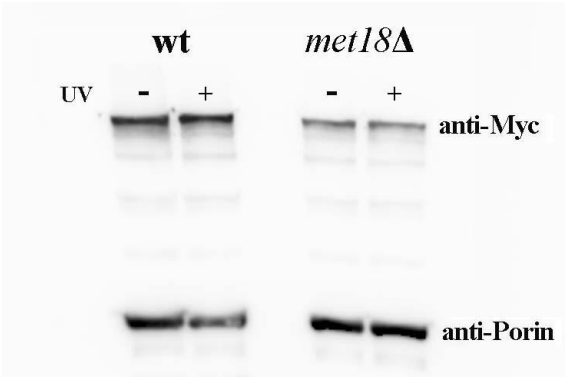

Figure 13: Western blot examination of the expression of the Rad3.9myc protein in WT (Rad3.9Myc) or *met18*Δ (*met18*ΔRad3.9Myc) and analysis on a 10% polyacrylamide gel. The picture was taken by exposure by the Las-3000(Fujifilm) following ECL treatment for 4min.The membrane was incubated with anti-porin as a protein loading control. The plus (+) and the minus (-) indicate the cells treated or not with 200j/m^2 UV irradiation (UV irradiation was done in cells suspended in25ml ddH20) and rested for recovery and activation of the NER pathway for 1h.

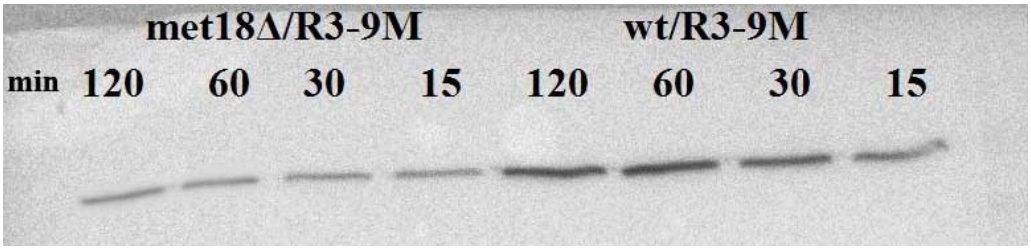

Figure 14: Western blot checking the expression of the Rad3.9myc protein in WT (Rad3.9Myc) or *met18*Δ (*met18*ΔRad3.9Myc) was analyzed on a 10% polyacrylamide gel. The picture was taken by exposure by the Las-3000 (Fujifilm) following ECL treatment for 4min. 15, 30, 60, 120 indicate the time post UV irradiation. The UV treatment was done by the same methodology as in ChIP experiment (200j/m^2 UV irradiation in25ml ddH20).

From **Figures 13 and 14** we can conclude that, the levels of Rad3 protein were affected by Met18 depletion but were not affected by UV irradiation. There was not a significant change in Rad3 protein levels between the different time points post UV irradiation in either strain (WT, *met18Δ*).

mRNA levels of Rad3 gene targets were reduced in *met18*Δ strain

Since we have found that binding of Rad3 was reduced in the *met18*Δ strain we further assessed, whether the expression of these target genes were also decreased in the mutant strain in native conditions and in conditions of UV irradiation (same treatment as for ChIP experiments).

In order to assess the role of Met18 in transcription and/or NER, the WT and the strain with disrupted the expression of Met18 (*met18*Δ) were treated with UV irradiation, in order to activate the NER pathway. After the UV treatment, the recovery of the cells for specific time point was done (the same time point of recovery examined during ChIP experiment (1h post UV irradiation), in order to accomplish repair. Then RNA was extracted from the aforementioned cells via Phenol/freeze protocol (described in materials and methods). After DNase treatment and cDNA synthesis by reverse transcription, the expression levels of Rad3 targets (*ADH1, PYK1*) were examined in all the aforementioned conditions by RT-Q-PCR. *GAL1* was used as a negative control.

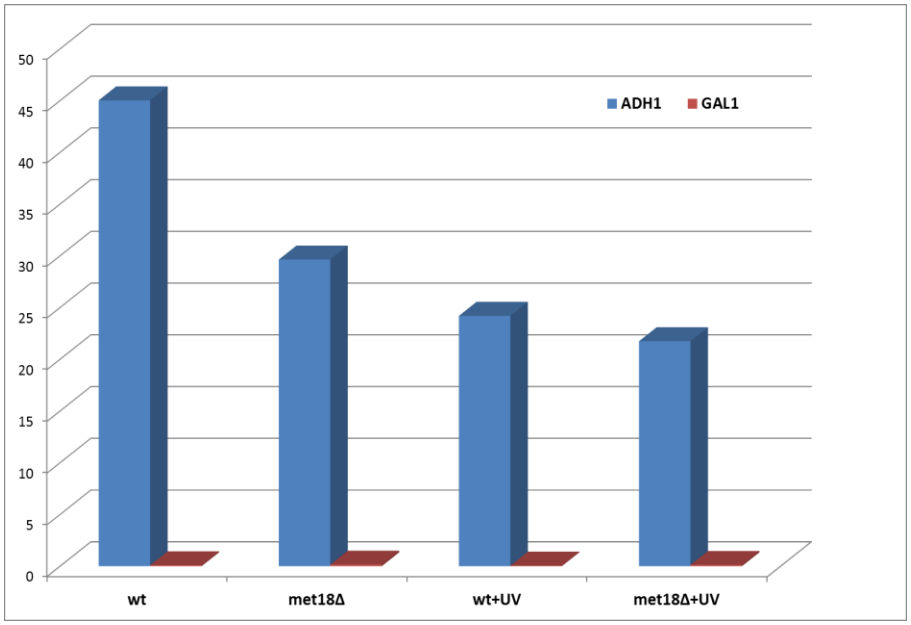

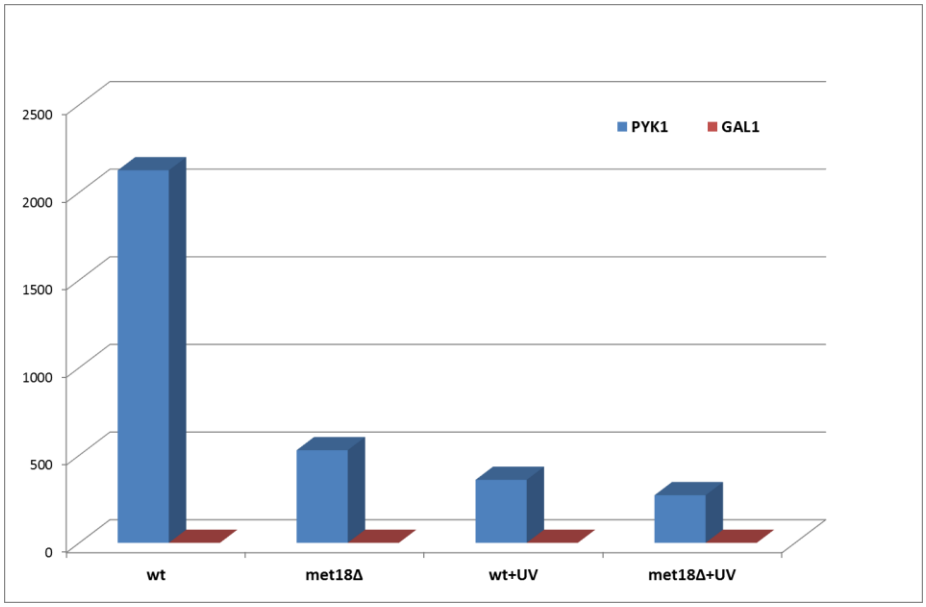

Figure 15: mRNA levels of *ADH1* and *PYK1* genes (Plot1 and plot2) blue bars in WT, *met18*Δ, WT cells treated with UV and *met18*Δ cells treated with UV. *GAL1*gene (red bars) was used as a negative control.

In both plots presented in **Figure 15** the mRNA levels of the genes presented were significantly decreased upon Met18 depletion compared to the WT. Upon UV irradiation there was also a slight decrease in the expression of the same genes compared to native conditions (YPD).Maximum mRNA decrease was observed upon both *MET18* deletion and UV treatment. This result is positively correlated with the results about the effect of Met18 depletion and UV irradiation on the recruitment of Rad3 on the promoters of the same examined genes (*ADH1* and *PYK1*).Therefore, Rad3 seems to positively affect transcription.

Is the physical interaction between Met18 and Rad3 affected upon genotoxic stress?

Physical interaction between Met18 and Rad3 proteins is known and conserved between yeast and mammals [48][46] . We were iterated to examine the same interaction under DNA damaging conditions and investigate possible alterations of the overall proteome related to Met18 and Rad9. For that we constructed a strain with tagged both Met18 and Rad3 with different epitopes. This strain is the Rad3.3HA, Met18.9Myc. As a control strain we would use the singly tagged Rad3.3HA. The same methodology used for the tagging and the disruption of Met18 was used for the construction of these strains. The PCR product corresponding to Rad3.3HA was inserted to the Met18.9Myc and to WT (FT5) strains via yeast transformation assay. Verification of both strains (Met18.9MycRad3.3HA, Rad3.3HA) was performed at both DNA and protein levels by diagnostic PCR and Western blot respectively (**Figure 16**).

a b c

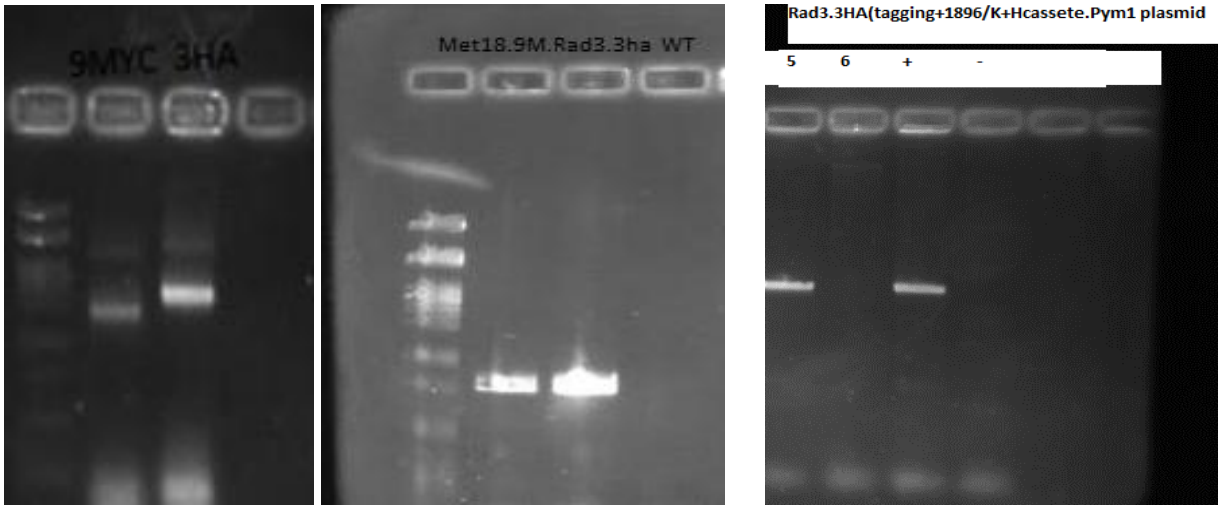

d

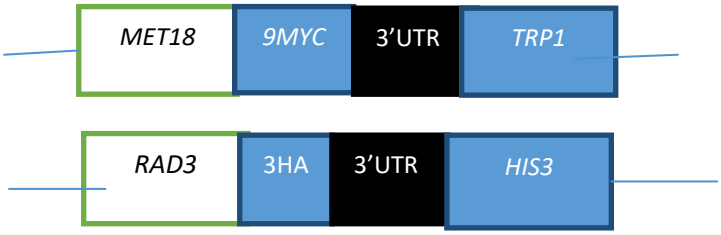

Figure 16: In the first 1,5% agarose gel 1λ of the PCR products used for the tagging of Met18 and Rad3 are presented. b) In the second gel the verification of Rad3 tagging in Met18.9Myc strain was done by PCR with primers specific for the sequence of Rad3 and for the sequence of the selection marker corresponding to the sequence of the tag 3HA. d) In the third gel the verification of Rad3 tagging in FT5 strain was done by PCR with primers specific for the sequence of Rad3 and for the sequence of the selection marker corresponding to the sequence of the tag 3HA. Positive construct is the Met18.9MycRad3.3HA strain. As negative control WT strain was used. d) The constructs of linear PCR products used for transformation containing *MET18*ORF, 9Myc tag, *MET18*3'UTR and *TRP1*gene for auxotrophy selection marker are presented.

Construction of Radioalabelled probes checking the Loxp site integration in MMS19 genomic locus

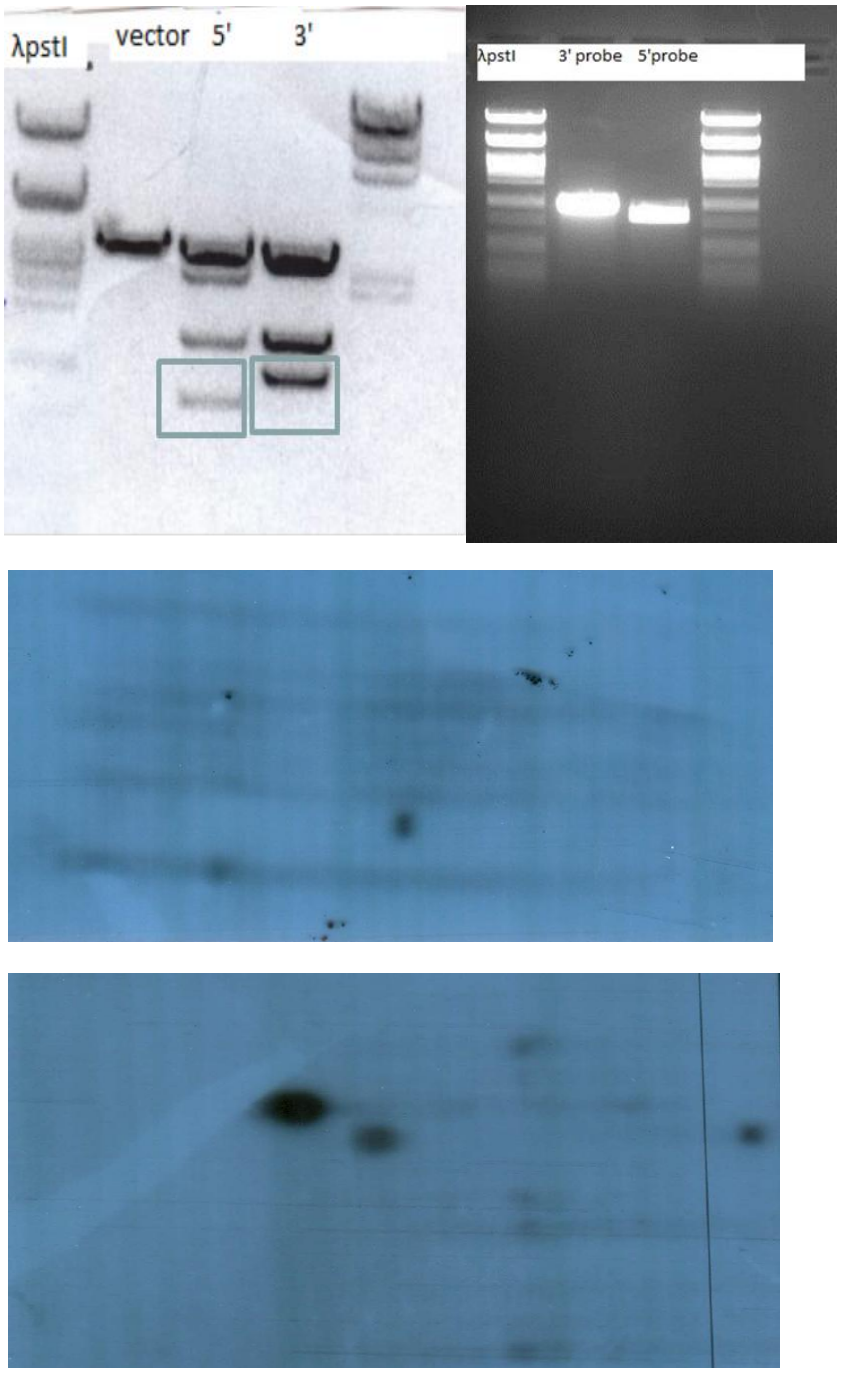

Figure 17: In the first agarose gel the targeting vector was cut with different restriction enzymes for the production of the radiolabeled probes. The uncut vector was used as a control. The bands in the boxes are the ones that were cut and further used for gel extraction. In the 3rd and 4th images Southern blot on XAB2 membrane was done in order to check the efficiency of the probe

Discussion

At present, any mechanistic understanding of how MMS19 functions in transcription and DNA repair remains elusive. Moreover, the pleiotropic outcomes driven by MMS19 defect are solely addressed to its role in the iron-sulfur metabolism, or the protein has additional functions?

In order to answer to the aforementioned questions, we develop a comprehensive and multidisciplinary approach to dissect the functional contribution of MMS19 in genome maintenance and gene expression regulation.

As far as uncovering the functional role of MMS19 in mouse models, Professor Garinis lab has recently generated Mmms19-/- mice; the mice were lethal at an early embryonic stage (Iamartino et al., unpublished results). For this purpose we generated ES cells for tissue specificMMS19 knock out animals for via the cre/flox system.

The experimental strategy followed for this purpose was the following: Firstly, electroporation with the specific expression vector containing the MMS19 genomic region (1st exon) flanked by two LoxP sites and a neo cassette (also flanked by to LoxP sites) which was already developed in Garinis lab (see materials and methods) was done in ES cells. After the first selection in selection media, genomic DNA was extracted from 197 clones and used for genotyping by PCR, checking the appropriate integration of the LoxP sites in the genomic locus of interest/MMS19, via homologous recombination and not in nonspecific region. The homologous recombination was further checked via Southern blots, with radiolabeled probes corresponding to the genomic sequence of MMS19.

We ended up with 65 clones positive for the integration of the LoxP site meaning that the electroporation efficiency was 33%.

To further examine the homologous recombination event by Southern blots, we managed to develop radiolabeled probes corresponding to the genomic sequence of MMS19 by the random priming method and with DNA template isolated by gel extraction corresponding to specific regions of the vector cut by restriction enzymes. These probes will be further used for the validation of the transformed ES cells. The positively transformed cells will be checked by karyotyping for the number of chromosomes in order to check whether the DNA construct with which they were transformed has resulted in chromosomal abnormalities. After checking these parameters the ES clones with the appropriate characteristics will be injected in blastocytes and these inserted into female pseudopregnant mice. Our aim is to generate tissue specific knock-out mouse following the crossing of the knock-in mouse (MMS19 $^{fl/fl}$) with a Cre mouse.

The development of this new model animal aims at a comprehensive study about the possible phenotypic changes resulted from the depletion of MMS19. Another aspect of the study could be the testing of possible transcriptome alterations with micro-array or RNA-seq assays and compare those results with published data, related to other NER defective mice models and or other specific transcription factor defective animals, whose outcomes resemble those produced by MMS19 depletion.

It has been difficult to dissect the functional contributions of NER factors in an intact mammalian organism. The budding yeast *Saccharomyces cerevisiae* offers a more versatile and well-developed platform to uncover pathways or screen for direct protein interactions beyond the descriptive level. For this reason in collaboration with Professor Alexandraki's lab we have used the *S. cerevisiae* to dissect the functional contribution of MMS19 (Met18) in DNA repair and transcription. To do this, we developed appropriately tagged and disrupted versions of Met18 in yeast cells and grew them under physiological conditions or under genotoxic stress including UV irradiation. Exploiting the known Met18 and Rad3 protein interaction (SGD) we also explored Met18 role in transcription by studying its effect on Rad3 recruitment to its known gene targets and testing whether met18 has the same gene targets. We also examined the effect of met18 depletion on Rad3 protein levels and its role in the expression of Rad3 targets. We examined Met18 recruitment to the known targets of Rad3 under native and DNA damaging conditions. We concluded that Met18 does not bind these Rad3 targets under all conditions used (native, UV irradiation, Zeocin treatment) (**Figure 10**).

There is controversial literature about the intracellular localization of Met18 and its homologue MMS19. According to older literature MMS19 protein localization was nuclear in mammals [55]. More recent studies indicated that it is only in the cytosol and its interaction with XPD takes place only in the cytosol[50]. As far as yeast is concerned there was not a fractionation study to examine the subcellular localization of Met18 and it was not known whether genotoxic stress can result in the movement of Met18 from the cytosol to the nucleus. According to high throughput imaging experiments in native conditions Met18-GFP is cytosolic (Cyclops database).The fact that Met18 does not bind to a known target of Rad3 may mean that they are not in a stable complex on chromatin or it could mean that Met18 has different gene targets than Rad3. In order to examine the aforementioned cases we could do genome-wide ChIP-seq experiments from Met18.9Myc strain in native conditions and in conditions of genotoxic stress. However, according to the recently resolved biochemical role of Met18 (MMS19) in the Fe-S addition pathway, the safest explanation of Met18 involvement in NER is that it is responsible for the addition of Fe-S cluster on Rad3 protein (NER protein) which occurs in the cytoplasm.

Met18 depletion is known to affect the Fe-S incorporation in different proteins with various functions including Rad3[48]. It was not known whether this results in decreased functionality of Rad3 protein. Rad3 except from its role in NER as a helicase is part of the general transcription factor TFIIH and takes part in transcription. So we examined the effect of Met18 depletion in the functionality of Rad3 by checking the effect of its depletion in the recruitment of Rad3 to its known targets in native conditions and in DNA damage conditions. It seems that Met18 depletion alone decreases the recruitment of the Rad3 to the promoters of the examined gene targets. Also the DNA damaging conditions lead to impaired recruitment of Rad3. Under both conditions the effect seems to be more severe (synergistic), meaning that UV treatment has stronger effect when Met18 is deleted (**Figure12**). That could mean that Met18 depletion and UV radiation affect Rad3 chromatin recruitment differently. For instance, UV may cause alterations in the Rad3 localization sites in the whole genome while Met18 depletion may affect protein levels (stability), functionality, structural changes and protein interactions of Rad3. Examination of Rad3 protein levels showed that UV irradiation does not affect the stability of the protein as its protein levels are not affected at all examined time points following exposure (**Figure 13 and Figure 14**) but the depletion of Met18 decreases significantly the protein levels of Rad3. Reduced levels may result from protein instability due to decreased addition of Fe-S cluster. This is in agreement with our above mentioned hypothesis and the literature on the relationship of the two proteins.

Finally, since we have found that the binding of Rad3 is affected in the *met18*Δ strain we also examined whether the expression of these gene targets was also decreased in the mutant strain in native conditions and following UV irradiation (same treatment as ChIP experiments).Examination of the specific gene RNA accumulation showed decreased expression levels of both *PYK1* and *ADH1* genes under both conditions, emphasizing the role of Rad3 in the transcription of these genes (**Figure 15**).From all the previous results we can conclude that Met18 depletion affects both the quantity (stability) of Rad3 protein and its functionality in transcription, not only its recruitment to its known targets, but also accumulation of their RNA.

In order to reveal the general effect of Met18 depletion on the genome-wide Rad3 recruitment and transcriptional role we could do ChIP sequencing experiments and RNA-seq from the WT and *met18*Δ strains.

Proteins interacting with MMS19 and Met18 are known by Mass spectrometric experiments. The effect of UV irradiation at the interactome of Met18 is not known. For this purpose we constructed a strain doubly tagged for Met18 and Rad3 (**Figure 16**). We can examine whether the known stable interaction between Met18 and Rad3 is affected upon genotoxic stress and more specifically by UV irradiation. The

effect of UV irradiation to the entire interactome of Met18could be performed by co-immunoprecipitation experiments followed by Mass spectrometry. The findings of these experiments could be further assessed in the mouse model.

The study of XPD and Rad3 is very important since both TFIIH mutation and Fe-S biosynthesis abnormalities can result in severe disease Syndromes such as xeroderma pigmentosum (XP), Cockayne syndrome (CS), trichothiodystrophy (TTD) and Fanconi anemia.

References

1. Sander M, Cadet J, Casciano DA, Galloway SM, Marnett LJ, Novak RF, et al. Proceedings of a workshop on DNA adducts: Biological significance and applications to risk assessment Washington, DC, April 13-14, 2004. Toxicology and Applied Pharmacology. 2005. pp. 1–20. doi:10.1016/j.taap.2004.12.012

2. Lindahl T. Instability and decay of the primary structure of DNA. Nature. 1993;362: 709–715. doi:10.1038/362709a0

3. Garinis G a, van der Horst GTJ, Vijg J, Hoeijmakers JHJ. DNA damage and ageing: new-age ideas for an age-old problem. Nat Cell Biol. 2008;10: 1241–1247. doi:10.1038/ncb1108-1241

4. Kamileri I, Karakasilioti I, Garinis GA. Nucleotide excision repair: New tricks with old bricks. Trends in Genetics. 2012. pp. 566–573. doi:10.1016/j.tig.2012.06.004

5. Partridge L, Gems D. Mechanisms of ageing: public or private? Nat Rev Genet. 2002;3: 165–175. doi:10.1038/nrg753

6. Harper JW, Elledge SJ. The DNA Damage Response: Ten Years After. Mol Cell. 2007;28: 739–745. doi:10.1016/j.molcel.2007.11.015

7. Hoeijmakers JHJ. Genome maintenance mechanisms are critical for preventing cancer as well as other aging-associated diseases. Mech Ageing Dev. 2007;128: 460–462. doi:10.1016/j.mad.2007.05.002

8. De Bont R, van Larebeke N. Endogenous DNA damage in humans: A review of quantitative data. Mutagenesis. 2004. pp. 169–185. doi:10.1093/mutage/geh025

9. Satya Prakash LP. Nucleotide excision repair in yeast. Mutat Res. 2000;45: 13–24. Available: http://www.sciencedirect.com/science?_ob=ArticleURL&_udi=B6T2C-40T9GVS-2&_user=2459786&_coverDate=06%2F30%2F2000&_rdoc=1&_fmt=&_orig=search&_sort=d&view=c&_acct=C000057396&_version=1&_urlVersion=0&_userid=2459786&md5=a1e31fbed6b676e89cd5444b5bd90ad0

10. Prakash L, Prakash S. Three additional genes involved in pyrimidine dimer removal in Saccharomyces cerevisiae: RAD7, RAD14 and MMS19. MGG Mol Gen Genet. 1979;176: 351–359. doi:10.1007/BF00333097

11. LeJeune D, Chen X, Ruggiero C, Berryhill S, Ding B, Li S. Yeast Elc1 plays an important role in global genomic repair but not in transcription coupled repair. DNA Repair (Amst). 2009;8: 40–50. doi:10.1016/j.dnarep.2008.08.010

12. Guzder SN, Sung P, Prakash L, Prakash S. Yeast RAD7-RAD16 complex, specific for the nucleotide excision repair of the nontranscribed DNA strand, is an ATP-dependent DNA damage sensor. J Biol Chem. 1997;272: 21665–21668. doi:10.1074/jbc.272.35.21665

13. Guzder SN, Sung P, Prakash L, Prakash S. The DNA-dependent ATPase activity of yeast nucleotide excision repair factor 4 and its role in DNA damage recognition. J Biol Chem. 1998;273: 6292–6296. doi:10.1074/jbc.273.11.6292

14. Fisher RP. Secrets of a double agent: CDK7 in cell-cycle control and transcription. J Cell Sci. 2005;118: 5171–5180. doi:10.1242/jcs.02718

15. Zurita M, Merino C. The transcriptional complexity of the TFIIH complex. Trends in Genetics. 2003. pp. 578–584. doi:10.1016/j.tig.2003.08.005

16. No Title.

17. Egly JM, Coin F. A history of TFIIH: Two decades of molecular biology on a pivotal transcription/repair factor. DNA Repair. 2011. pp. 714–721. doi:10.1016/j.dnarep.2011.04.021

18. Giglia-Mari G, Coin F, Ranish J a, Hoogstraten D, Theil A, Wijgers N, et al. A new, tenth subunit of TFIIH is responsible for the DNA repair syndrome trichothiodystrophy group A. Nat Genet. 2004;36: 714–719. doi:10.1038/ng1387

19. No Title.

20. Moreland RJ, Tirode F, Yan Q, Conaway JW, Egly JM, Conaway RC. A role for the TFIIH XPB DNA helicase in promoter escape by RNA polymerase II. J Biol Chem. 1999;274: 22127–22130. doi:10.1074/jbc.274.32.22127

21. Dvir A, Conaway JW, Conaway RC. Mechanism of transcription initiation and promoter escape by RNA polymerase II. Current Opinion in Genetics and Development. 2001. pp. 209–214. doi:10.1016/S0959-437X(00)00181-7

22. Yudkovsky N, Ranish JA, Hahn S. A transcription reinitiation intermediate that is stabilized by activator. Nature. 2000;408: 225–229. doi:10.1038/35041603

23. Rossignol M, Kolb-Cheynel I, Egly JM. Substrate specificity of the cdk-activating kinase (CAK) is altered upon association with TFIIH. EMBO J. 1997;16: 1628–1637. doi:10.1093/emboj/16.7.1628

24. Yankulov KY, Bentley DL. Regulation of CDK7 substrate specificity by MAT1 and TFIIH. EMBO J. 1997;16: 1638–1646. doi:10.1093/emboj/16.7.1638

25. Akhtar MS, Heidemann M, Tietjen JR, Zhang DW, Chapman RD, Eick D, et al. TFIIH Kinase Places Bivalent Marks on the Carboxy-Terminal Domain of RNA Polymerase II. Mol Cell. 2009;34: 387–393. doi:10.1016/j.molcel.2009.04.016

26. Okhuma Y, Roeder RG. Regulation of TFIIH ATPase and kinase activities by TFIIE during active initiation complex formation. Nature. 1994;368: 160–163. doi:10.1038/368160a0

27. Akoulitchev S, Chuikov S, Reinberg D. TFIIH is negatively regulated by cdk8-containing mediator complexes. Nature. 2000;407: 102–106. doi:10.1038/35024111

28. Iben S, Tschochner H, Bier M, Hoogstraten D, Hoz??k P, Egly JM, et al. TFIIH plays an essential role in RNA polymerase I transcription. Cell. 2002;109: 297–306. doi:10.1016/S0092-8674(02)00729-8

29. Hoogstraten D, Nigg AL, Heath H, Mullenders LHF, Van Driel R, Hoeijmakers JHJ, et al. Rapid switching of TFIIH between RNA polymerase I and II transcription and DNA repair in vivo. Mol Cell. 2002;10: 1163–1174. doi:10.1016/S1097-2765(02)00709-8

30. Oksenych V, de Jesus BB, Zhovmer A, Egly J-M, Coin F. Molecular insights into the recruitment of TFIIH to sites of DNA damage. EMBO J. 2009;28: 2971–2980. doi:10.1038/emboj.2009.230

31. Giglia-Mari G, Miquel C, Theil AF, Mari PO, Hoogstraten D, Ng JMY, et al. Dynamic interaction of TTDA with TFIIH is stabilized by nucleotide excision repair in living cells. PLoS Biol. 2006;4: 0952–0963. doi:10.1371/journal.pbio.0040156

32. Dubaele S, De Santis LP, Bienstock RJ, Keriel A, Stefanini M, Van Houten B, et al. Basal transcription defect discriminates between xeroderma pigmentosum and trichothiodystrophy in XPD patients. Mol Cell. 2003;11: 1635–1646. doi:10.1016/S1097-2765(03)00182-5

33. Chen J, Larochelle S, Li X, Suter B. Xpd/Ercc2 regulates CAK activity and mitotic progression. Nature. 2003;424: 228–232. doi:10.1038/nature01746

34. Li X, Urwyler O, Suter B. Drosophila Xpd regulates Cdk7 localization, mitotic kinase activity, spindle dynamics, and chromosome segregation. PLoS Genet. 2010;6. doi:10.1371/journal.pgen.1000876

35. Ito S, Tan LJ, Andoh D, Narita T, Seki M, Hirano Y, et al. MMXD, a TFIIH-Independent XPD-MMS19 Protein Complex Involved in Chromosome Segregation. Mol Cell. 2010;39: 632–640. doi:10.1016/j.molcel.2010.07.029

36. Fousteri M, Mullenders LHF. Transcription-coupled nucleotide excision repair in mammalian cells: molecular mechanisms and biological effects. Cell Res. 2008;18: 73–84. doi:10.1038/cr.2008.6

37. Hanawalt PC, Spivak G. Transcription-coupled DNA repair: two decades of progress and surprises. Nat Rev Mol Cell Biol. 2008;9: 958–970. doi:10.1038/nrm2549

38. Li S, Smerdon MJ. Rpb4 and Rpb9 mediate subpathways of transcription-coupled DNA repair in Saccharomyces cerevisiae. EMBO J. 2002;21: 5921–5929. doi:10.1093/emboj/cdf589

39. Li S, Chen X, Ruggiero C, Ding B, Smerdon MJ. Modulation of Rad26- and Rpb9-mediated DNA repair by different promoter elements. J Biol Chem. 2006;281: 36643–36651. doi:10.1074/jbc.M604885200

40. Sharma AK, Pallesen LJ, Spang RJ, Walden WE. Cytosolic iron-sulfur cluster assembly (CIA) system: Factors, mechanism, and relevance to cellular iron regulation. Journal of Biological Chemistry. 2010. pp. 26745–26751. doi:10.1074/jbc.R110.122218

41. Van Wietmarschen N, Moradian A, Morin GB, Lansdorp PM, Uringa EJ. The mammalian proteins MMS19, MIP18, and ANT2 are involved in cytoplasmic iron-sulfur cluster protein assembly. J Biol Chem. 2012;287: 43351–43358. doi:10.1074/jbc.M112.431270

42. Queimado L, Rao M, Schultz RA, Koonin E V, Aravind L, Nardo T, et al. Cloning the human and mouse MMS19 genes and functional complementation of a yeast mms19 deletion mutant. Nucleic Acids Res. 2001;29: 1884–1891.

43. Askree SH, Yehuda T, Smolikov S, Gurevich R, Hawk J, Coker C, et al. A genome-wide screen for Saccharomyces cerevisiae deletion mutants that affect telomere length. Proc Natl Acad Sci U S A. 2004;101: 8658–63. doi:10.1073/pnas.0401263101

44. Kou H, Zhou Y, Gorospe RMC, Wang Z. Mms19 protein functions in nucleotide excision repair by sustaining an adequate cellular concentration of the TFIIH component Rad3. Proc Natl Acad Sci U S A. 2008;105: 15714–15719. doi:10.1073/pnas.0710736105

45. Lombaerts M, Tijsterman M, Verhage RA, Brouwer J. Saccharomyces cerevisiae mms19 mutants are deficient in transcription-coupled and global nucleotide excision repair. Nucleic Acids Res. 1997;25: 3974–3979. doi:10.1093/nar/25.20.3974

46. Stehling O, Vashisht AA, Mascarenhas J, Jonsson ZO, Sharma T, Netz DJ, et al. {MMS19} assembles iron-sulfur proteins required for {DNA} metabolism and genomic integrity. Science (80-). 2012;337: 195–199. doi:10.1126/science.1219723

47. Lev I, Volpe M, Goor L, Levinton N, Emuna L, Ben-Aroya S. Reverse PCA, a Systematic Approach for Identifying Genes Important for the Physical Interaction between Protein Pairs. PLoS Genet. 2013;9. doi:10.1371/journal.pgen.1003838

48. Gari K, León Ortiz AM, Borel V, Flynn H, Skehel JM, Boulton SJ. MMS19 links cytoplasmic iron-sulfur cluster assembly to DNA metabolism. Science. 2012;337: 243–5. doi:10.1126/science.1219664

49. Li F, Martienssen R, Cande WZ. Coordination of DNA replication and histone modification by the Rik1-Dos2 complex. Nature. 2011;475: 244–8. doi:10.1038/nature10161

50. Vashisht AA, Yu CC, Sharma T, Ro K, Wohlschlegel JA. The association of the xeroderma pigmentosum group D DNA helicase (XPD) with transcription factor IIH is regulated by the cytosolic iron-sulfur cluster assembly pathway. J Biol Chem. 2015;290: 14218–14225. doi:10.1074/jbc.M115.650762

51. Moiseeva TN, Gamper AM, Hood BL, Conrads TP, Bakkenist CJ. Human DNA polymerase ε is phosphorylated at serine-1940 after DNA damage and interacts with the iron-sulfur complex chaperones CIAO1 and MMS19. DNA Repair (Amst). 2016;43: 9–17. doi:10.1016/j.dnarep.2016.04.007

52. Jain R, Vanamee ES, Dzikovski BG, Buku A, Johnson RE, Prakash L, et al. An iron-sulfur cluster in the polymerase domain of yeast DNA polymerase ε. J Mol Biol. 2014;426: 301–308. doi:10.1016/j.jmb.2013.10.015

53. Wang Z, Wu X, Friedberg EC. DNA repair synthesis during base excision repair in vitro is catalyzed by DNA polymerase epsilon and is influenced by DNA polymerases DNA Repair Synthesis during Base Excision Repair In Vitro Is Catalyzed by DNA Polymerase E and Is Influenced by DNA Polym. Mol Cell Biol. 1993;13: 1051–1058. doi:10.1128/MCB.13.2.1051.Updated

54. Shivji MK, Podust VN, Hübscher U, Wood RD. Nucleotide excision repair DNA synthesis by DNA polymerase epsilon in the presence of PCNA, RFC, and RPA. Biochemistry. 1995;34: 5011–7. Available: http://www.ncbi.nlm.nih.gov/pubmed/7711023

55. Seroz T, Winkler GS, Auriol J, Verhage RA, Vermeulen W, Smit B, et al. Cloning of a human homolog of the yeast nucleotide excision repair gene MMS19 and interaction with transcription repair factor TFIIH via the XPB and XPD helicases. Nucleic Acids Res. 2000;28: 4506–4513. doi:10.1093/nar/28.22.4506

56. Esnault C, Ghavi-Helm Y, Brun S, Soutourina J, Van Berkum N, Boschiero C, et al. Mediator-Dependent Recruitment of TFIIH Modules in Preinitiation Complex. Mol Cell. 2008;31: 337–346. doi:10.1016/j.molcel.2008.06.021